MARMARA UNIVERSITY
INSTITUTE OF GRADUATE STUDIES
IN PURE AND APPLIED SCIENCES

ADSORPTION OF CR (VI) IONS IN WASTEWATERS ON HYDROTHERMALLY SYNTHESIZED CHITOSAN/POLYVINYL ALCOHOL BEADS IN CONTINUOUS SYSTEMS

Eylül KÖSOĞLU

MASTER THESIS
Department of Chemical Engineering

THESIS SUPERVISOR
Assoc. Prof. Dr. Yaşar Andelib AYDIN

ISTANBUL, 2023

MARMARA UNIVERSITY
INSTITUTE OF GRADUATE STUDIES
IN PURE AND APPLIED SCIENCES

ADSORPTION OF CR(VI) IONS IN WASTEWATERS ON HYDROTHERMALLY SYNTHESIZED CHITOSAN/POLYVINYL ALCOHOL BEADS IN CONTINUOUS SYSTEMS

Eylül KÖSOĞLU

(524520008)

MASTER THESIS
Department of Chemical Engineering

THESIS SUPERVISOR
Assoc. Prof. Dr. Yaşar Andelib AYDIN

ISTANBUL, 2023

ACKNOWLEDGEMENT

Words cannot express my gratitude to my advisor, Assoc. Prof. Dr. Yaşar Andelib AYDIN, who shared her valuable knowledge, experience and wisdom with me, and supported me with patience and great interest whenever I consulted her for my thesis. I would like to extend my thanks to my dear family, who have always been by my side for their moral and material support throughout my entire life. I would also like to thank to Prof. Dr. Atıf KOCA, Assoc. Prof. Dr. Neslihan Alemdar YAYLA and Assoc. Prof. Dr. Özge KERKEZ KUYUMCU for allowing me to use the laboratory facilities. Also I would like to thank my friend Asude Sena DEMİRCİ ÜLKE for the contribution of the information I gained from her previous works to this project. Lastly, I would like to mention The Scientific And Technological Research Council Of Turkey (TUBITAK) for supporting this Project financially with Project number 222M367.

Eylül KÖSOĞLU

Chemical Engineer

June, 2023

TABLE OF CONTENTS

HİDROTERMAL YÖNTEM İLE SENTEZLENMİŞ KİTOSAN-POLİVİNİL ALKOL ADSORBAN BONCUKLARI İLE SABİT YATAKLI KOLONDA CR (VI) ADSORPSİYONU

ÖZET

Endüstriyel atıkların deşarjı nedeniyle su kaynaklarının kirlenmesi, önemli bir çevre sorunudur. Endüstriyel atık sularda fazla miktarda ağır metal iyonları ve organik kirleticiler bulunması insan sağlığını ve çevreyi tehlikeye atabilir. Sulu çözeltilerde bulunan ağır metallerin uzaklaştırılması için kimyasal çöktürme, iyon değişimi, filtrasyon, membran teknolojileri, oksidasyon-indirgeme işlemi, diyaliz, elektrodiyaliz ve elektrolitik ekstraksiyon dahil olmak üzere çeşitli yöntemler geliştirilmiş ve uygulanmıştır.

Cr (VI), endüstriyel atıksularda yaygın olarak bulunan ağır metallerden biri olup, insan ve diğer canlılara zararlı, kanserojen ve toksik bir kirleticidir. Bu nedenle atıksulardan krom giderimi için verimliliği yüksek yöntemlerin ve/veya etkin giderim sağlayan malzemelerin geliştirilmesi önem taşımaktadır. Bu tez kapsamında atıksulardan krom gideriminde kullanılmak üzere düşük maliyetli, uygulama kolaylığı sağlayan ve çevre dostu bir adsorban yapı geliştirilmesi hedeflenmiş ve yapının giderim performansı sabit yataklı sürekli adsorpsiyon kolonunda kullanılarak uygun modeller çerçevesinde incelenmiştir.

Atık sudan yüksek verim ile ağır metal giderimi sağlayabilen doğal polimerler arasında kitosan, toksik olmaması, biyolojik olarak parçalanabilirliği, geniş doğal kaynağı ve biyoaktif özellikleri sayesinde adsorban olarak oldukça iyi bir seçenektir. Kitosan içerdiği $-NH_2$ ve -OH fonksiyonel grupları sayesinde modifiye edilebilir bir yapıdadır. Modifikasyon neticesinde, hidrofilik özellik, mekanik mukavemet ve yapısal kararlılık gibi özellikleri uyarlanabilmektedir. Modifikasyon için kullanılabilecek en önemli polimerlerden biri toksik olmaması, kolay bulunabilirliği ve düşük maliyeti sayesinde polivinil alkoldür. Kitosan polivinil alkol karışım polimerlerinin asidik ortamdaki çözünürlüğü adğır metal adsorpsiyonunda değerlendirilmesini kıstlamaktadır. Bu amaçla uygulanan Çapraz bağlama reaksiyonları yapının aktif –OH ve –NH2 grupları üzerinden gerçekleştiğinden adsorpsiyon kapasitesini düşürür.

Ancak yüksek basınç ve sıcaklıkta yürütülen hidrotermal yöntemin fiziksel çapraz bağlama sağladığı ve adsorpsiyon kapasitesini artırma yönünde etki ettiği önceki çalışmalarla ispatlanmıştır.

Bu çalışmada 140 ˚C, 12 saat koşullarında gerçekleştirilen hidrotermal yöntem ile çapraz bağlanmış kitosan/polivinil alkol boncukları sabit yataklı kolonda dolgu malzemesi olarak kullanılmış ve sürekli koşullarda Cr (VI) giderimi gerçekleştirilmiştir. Yatak yüksekliği, başlangıç konsantrasyonu, akış hızı gibi çeşitli parametreler 2,5-7,5 ml/dk, 20-60 ppm ve 2-6 cm aralıklarında değiştirilerek, adsorpsiyon kapasitesi hesaplanmıştır. Uygulanan sürekli adsorpsiyon sonucunda elde edilen veri seti kullanılarak kırılım eğrileri çizilmiş ve Yoon Nelson, Adams Bohart, Thomas, BDST (Bed Depth Service Time) modellerine uygunluğu araştırılmıştır. Model katsayıları doğrusal olmayan regresyon analizi ile belirlenmiştir.

Polivinil alkol (PVA) ve kitosandan (CS) oluşan, kompozit hidrojel boncuklarının, yüzey alanları ve gözeneklilikleri azot adsorpsiyonu (BET) analizi ile belirlenmiştir. Yüzey özellikleri taramalı elektron mikroskobu (SEM) ile görselleştirilmiş, adsorbanın fonksiyonel gruplarını karakterize etmek için Fourier Dönüşümlü Kızılötesi Spektroskopisi (FTIR) yöntemi kullanılmıştır. Ayrıca SEM-EDX analizi ile elemental bileşim tayini yapılmıştır.

Bu çalışma sonucunda, H-CS/PVA adsorbentinin sürekli koşullar altında da çalıştığı kanıtlanmış ve 15,53 mg/g adsorpsiyon kapasitesine ulaşılmıştır. Minimum giderim %23,12 olarak tespit edilirken, maksimum giderim %64,2'ye kadar ulaşmıştır. Çalışılan modeler arasında, Yoon-Nelson modeli sürekli sistemde H-CS/PVA üzerine Cr (VI) adsorpsiyonunun açıklanması için en tutarlı model olarak seçilmiştir. Bütün bu vargılar, CS/PVA boncuklarının çapraz bağlanması için hidrotermal işlemin kullanımını haklı çıkarmaktadır.

ADSORPTION OF CR(VI) IONS IN WASTEWATERS ON HYDROTHERMALLY SYNTHESIZED CHITOSAN/POLYVINYL ALCOHOL BEADS IN CONTINUOUS SYSTEMS

ABSTRACT

Important environmental problems arise as a result of industrial waste discharge to water resources. Excess heavy metal ions and organic pollutants in industrial wastewater can endanger human health and the environment. Conventional methods that have been established and employed for the elimination of heavy metals from aqueous media include chemical precipitation, ion exchange, filtration, membrane technologies, oxidation-reduction treatment, dialysis, electrodialysis and electrolytic extraction.

Cr (VI) is one of the heavy metals commonly found in industrial wastewater and is a carcinogenic and toxic pollutant that is harmful to humans and other living things. For this reason, it is important to develop methods with high efficiency and/or materials that provide effective removal for chromium removal from wastewater. Within the scope of this thesis, it is aimed to develop a low cost, easy to apply and environmentally friendly adsorbent structure to be used in the removal of chromium from wastewater, and the removal performance of the structure was examined within the framework of suitable models by using it in a fixed bed continuous adsorption column.

Among the natural polymers that can provide highly efficient heavy metal removal from wastewater, chitosan is a very good choice as an adsorbent thanks to its non-toxicity, biodegradability, wide natural resource and bioactive properties. Chitosan has a structure that can be modified thanks to the -NH_2 and -OH functional groups it contains. As a result of the modification, properties such as hydrophilic property, mechanical strength and structural stability can be adapted. One of the most important polymers that can be used for modification is polyvinyl alcohol due to its non-toxicity, easy availability and low cost. The solubility of chitosan polyvinyl alcohol blend polymers in acidic media limits their evaluation in heavy metal adsorption. The cross-linking reactions applied for this purpose reduce the adsorption capacity of the structure as it occurs over the active –OH and –NH_2 groups. However, it has been proven by previous studies that the hydrothermal method carried out at high pressure and temperature provides physical cross-linking and

has an effect on increasing the adsorption capacity.

In this study, H-CS/PVA (chitosan/polyvinyl alcohol beads cross-linked by hydrothermal method carried out at 140 ˚C, 12 hours) were used as filling material in the fixed bed column and Cr (VI) removal was carried out under continuous conditions. The adsorption capacity was calculated by changing various parameters such as bed height, initial concentration, and flow rate in the respective ranges of 2-6 cm, 20-60 ppm and 2.5-7.5 ml/min. The breakthrough curves were drawn using the data set gained as a result of continuous adsorption experiments. Nonlinear regression analysis was involved in the curve fitting procedure applied for Yoon-Nelson, Adams-Bohart, Thomas and BDST (Bed Depth Service Time) models. Model coefficients were determined, accordingly.

Surface area and porosity of hydrothermally treated beads were determined by nitrogen adsorption (BET) analysis. Surface properties were visualized by scanning electron microscopy (SEM), and Fourier Transform Infrared Spectroscopy (FTIR) method was used to characterize the functional groups of the adsorbent. In addition, elemental composition was determined by SEM-EDX analysis.

An adsorption capability of 15.53 mg/g has been accomplished with the H-CS/PVA adsorbent, and it has been demonstrated that it is also effective under continuous circumstances. The lowest percentage of removal that was found was 23.12%, while the highest percentage of removal that was found was 64.2%. Out of the studied models, Yoon-Nelson model was selected to be the most consistent one for describing the adsorption of Cr (VI) onto H-CS/PVA in continuous system. All these conclusions justified that the application of hydrothermal treatment for the cross-linking of CS/PVA beads was feasible.

SYMBOLS

C_0 : Initial Concentration (mg/l)

C_{ad} : Adsorbed Concentration (mg/l)

C_t : Effluent Concentration (mg/l)

h_{bed} : Bed height (cm)

k_{AB} : Adams-Bohart Kinetic Constant (ml/mg min)

k_{TH} : Thomas kinetic constant (ml/mg.min)

k_{YN} : Yoon-Nelson Kinetic Constant (l/min)

k_{BDST} : BDST Kinetic Constant (ml/mg.min)

m : Adsorbent Amount in the Column (g)

N_0 : Adsorption Capacity Per Unit Volume of Bed (mg/l)

Q : Flow Rate

q_{tot} : Total Adsorbate Amount

q_e : Uptake Capacity (mg/g)

τ : Time Required for 50% Adsorbate Breakthrough (min)

t_b : Breakthrough Time (min)

t_{tot} : Total flow time (min)

u : Linear Flow Rate (ml/cm^2 min)

U_0 : Linear Velocity (cm/min)

V_{eff} : Output volume (ml)

X^2 : Chi-square Test

Z_0 : Critical Bed Depth (cm)

ε : Percent Deviation (%)

ABBREVIATIONS

ARE : Average Relative Error

BC : Breakthrough Curve

BDST : Bed Depth Service Time

BET : Brunauer-Emmett-Teller

CS : Chitosan

EDX : Energy Dispersive X-Ray

FTIR : Fourier Transform Infrared Spectroscopy

H-CS/PVA: Hydrothermally Treated Chitosan/Polyviny Alcohol

MPSD : Marquardt's Percent Standard Deviation

MTZ : Mass Transfer Zone

PVA : Polyvinyl Alcohol

SEM : Scanning Electron Microscope

LIST OF FIGURES

LIST OF TABLE

1. INTRODUCTION

The rapidly increasing population and the development of industry have caused environmental pollution, and therefore the pollution of water resources. An important sources of this pollution is industrial wastewater. Heavy metals are amongst the most significant contributors to environmental pollution caused by industrial wastewater. Heavy metals, classified as micro-pollutants, are commonly employed in production and auxiliary processes in many industries. The majority of heavy metals are toxic to organisms and have a tendency to accumulate even at very low amounts, resulting in severe negative impacts on the environment and on organisms [1].

Remediation of heavy metal bearing water is important in terms of minimizing the damage to the environment and ensuring pollution control. Commonly applied methods used in the treatment of heavy metal-containing wastewater vary according to the type of heavy metal and the size of the treatment need. The development of new techniques that do not cause secondary pollution on the environment and that reduce operational costs has gained importance in recent years. Adsorption has been considered as an effective and efficient method that can eliminate many disadvantages associated with other common methods and in this respect, the studies on adsorption are adding up, continuously. A significant portion of the effort is devoted to utilization of low cost, widely available adsorbents of natural origin. [2] Among the natural adsorbent materials used activated carbon, fly ash, zeolites, clays, various plant wastes, chitin, chitosan can be listed [3].

Chitosan is used in the removal of many toxic heavy metals thanks to the contained functional amino and hydroxyl groups. However, when used as an adsorbent as it is, a number of limitations related to low specific gravity, high cost, and inferior mechanical properties need to be resolved [4]. For this reason, chitosan is modified in order to increase its chemical and physical resistance in practical applications.

Since chitosan is soluble in acidic pH conditions, strategies such as cross-linking, chemical modification and preparation of mixtures with different polymers should be applied to increase its mechanical and chemical resistance. In this context, polyvinyl alcohol is one of the most preferred polymers for the modification process due to its high biocompatibility, hydrophilic nature, superior mechanical strength and flexibility, thermal stability and non-toxicity, easy availability and low cost [5].

In this thesis, the adsorption of Cr (VI) ions to hydrothermally treated polyvinyl alcohol-modified chitosan adsorbent beads was studied in a fixed bed column system operated continuously. During the adsorption process, flow and column parameters, namely, flow rate (Q), feed concentration (C_0) and height of the adsorbent bed (h_{bed}), were changed and breakthrough curves specific to each of the applied process condition were established. The adsorption capacities of the beads were calculated under different conditions and the adsorption was characterized with a series of models used for dynamic modelling of the continuous adsorption columns.

1.1.Literature Review

When the literature is examined, it is seen that CS/PVA blend adsorbents can be used for the purification of various heavy metals from wastewater. Anitha et al. (2014) observed that Zn (II) ions were adsorbed on the CS/PVA mixture, resulting in a maximum adsorption of 99.45% [6]. In another study, polyethyleneimine (PEI) was introduced to chitosan/polyvinyl alcohol membrane structure aiming for increasing the number of amine groups and increasing the ionic metal adsorbent properties, concordantly. The adsorption capacity of CS/PVA/PEI membrane structure was determined to be 75.5, 86.08 and 112.13 mg/g for Ni^{2+} Cu^{2+} and $Cd^{2+,}$ ions at 25°C and pH 6, respectively [7]. Li et al. (2015) synthesized a bio-adsorbent by incorporating graphene oxide (GO) to CS/PVA blend hydrogel beads and determined that the maximum adsorption capacity (q_{max}) for Cu (II) was 162 mg/g at 30 °C [8]. In another study, Pb(II) adsorption was aimed using CS/PVA blend films and q_{max} was calculated as 7.67 mg/g [9]. In a study carried out within our research group, composite films with -OH and -NH_2 functional groups were fabricated from CS, PVA and carbon nanotubes doped with amine functionalities (a-MWCNT). The maximum Cr (VI) uptake capacity of the CS/PVA/a-MWCNT composite film was reported as 134.2 mg/g [10]. In all of these surveyed research works, the technique of chemical crosslinking was applied in order to ensure both the mechanical and physical durability. The several types of cross-linkers that were used are detailed in Table 1.1.

Table 1. 1. Results of previous studies with CS/PVA mixture and composite adsorbents in batch conditions

Sample Name	Morphological Structure	Cross-linker	Metal Ion	Adsorption Capacity (mg/g)	Reference
CS/PVA	Film	Glutaraldehyde	Zn (II)	7.816	[6]
CS/PVA/PEI	Membrane	Glutaraldehyde	Cu (II)	112.13	
	Membrane	Glutaraldehyde	Ni (II)	86.08	[7]
	Membrane	Glutaraldehyde	Cd (II)	75.5	
CS/PVA/GO	Bead	Boric Acid	Cu (II)	162	[8]
CS/PVA	Film	Glutaraldehyde	Pb (II)	7.67	[9]
CS/PVA/ a-MWCNT	Film	Glutaraldehyde	Cr (VI)	134.2	[10]
CS/PVA	Film	Glutaraldehyde	Cr (VI)	49.34	[10]
CS/PVA	Bead	Glutaraldehyde (1.325 mM) + Hydrothermal method	Cr (VI)	33.09	[11]
	Bead	Hydrothermal Method	Cr (VI)	80.89	[11]

Though chemical crosslinking assures satisfactory mechanical and physical endurance, it also leads to loss of active adsorption sites. Thus, the development of effective physical cross-linking procedures are required to eliminate the requirement for chemical cross-linking. CS/PVA blend can also be cross-linked by physical methods such as heat treatment, freeze-thawing and etc [12, 13].

Recently, Yi et al. (2020) have proposed hydrothermal treatment as a benefical method for increasing the Cr (VI) adsorption capacity of chitosan [14]. Concerning this fact, previous projects conducted in our research group aimed for employing the hydrothermal treatment technique in the synthesis of CS/PVA blend films and beads prior to batch adsorption of Cr (VI). As listed in the last two rows of Table 1.1, significant improvement was recorded in Cr (VI) adsorption capacity with respect to CS/PVA beads cross-linked with glutaraldehyde. Noteable enhancements were also detected in the surface area, pore

characteristics, chemical structure and mechanical durability when the treatment was conducted under optimal operation conditions of 140°C and 12 h. The results of these works clearly verified the effectiveness of hydrothermally treated CS/PVA beads in Cr (VI) adsorption.

All in all, this thesis aimed for the utilization of H-CS/PVA blend beads, cross-linked by the help of hydrothermal method, in a continuously operated adsorption column as the fixed-bed material to remove Cr (VI) heavy metal ions from wastewater. The modeling of column data was applied in order to assure adaptibility to large scale water purification.

1.2.Water Pollution and Wastewater

The environmental pollution has become an important issue in all over the world with the rapid increase in population, lack of energy and food, irregular urbanization, developing technology, and increasing industrialization to meet the demands of people. The industrialization and the increase in the demand for commodity products have caused a dramatic rise in the amount of wastewater and its heavy metal content.

Water pollution is defined as the discharge of substances or energy wastes that will degrade biological resources, human health, fisheries, and water quality through direct or indirect means. The primary indicators of water pollution are the adverse changes detected in the characteristics of the water source. Waste water emerges as water that has been polluted or whose properties have been partly or entirely changed due to domestic, industrial, agricultural and other uses such as mines and mineral processing facilities [15].

As long as the pollutants in domestic wastewater are not in excessive amounts, they can be converted into harmless inorganic compounds by microorganisms. Industrial wastewater shows significant differences when compared to domestic wastewater [16]. Persistent pollutants present in industrial wastewater have the property of accumulating and condensing in the tissues of organisms and creating a direct toxic effect when they are above certain amounts. In addition, as a result of pollution, the environmental balance can be irreversibly deteriorated [17].

Besides urban wastes and sewage waters, the wastewater of many industries, to which chemistry, food, textile, paper and leather can be noted as examples, are important sources of pollution in surface waters such as sea, lake and river. Waste water treatment has been

identified as a significant issue for the prevention of environmental pollution considering the massive amount and the anticipated concentration of effluent, and the large number of industries. Industrial waste water includes multifarious organic and inorganic pollutants in which heavy metals constitute an important fraction [18].

1.3. Heavy Metal Contamination in Wastewater

Heavy metals are a group of metals with densities higher than 5 g/cm^3, including lead, cadmium, chromium, nickel, mercury, and arsenic. They have different physical, chemical, and biological characteristics and may be toxic to living organisms over certain concentrations. Due to their chemical properties, heavy metals are common in many areas of our daily life. They are often found with other pollutants in wastewater from metal cleaning, metal plating, electroplating, iron and steel, auto parts, paint, printing, textile, petrochemical and leather industries [19]. Table 1.2 shows major metals found in wastewater.

Table 1. 2. Major toxic metals discharged into the aquatic environment from various industries [20]

Industry	Cd	Cr	Cu	Hg	Ni	Pb	Sn	Zn
Chlorine Alkali Production	+	+	-	+	-	+	+	+
Energy Production	+	+	+	+	+	+	+	+
Fertilizer	+	+	-	+	-	+	-	+
Iron-Steel	+	+	+	+	+	+	-	+
Paint and Pigment	+	+	+	-	+	+	-	+
Paper	-	+	+	+	+	+	-	-
Petrochemical	+	+	+	+	+	+	+	+

Heavy metals are transferred to rivers, lakes and underground waters by the discharge of industrial wastes or by acid rain eroding the soil, thus causing dissolution of the heavy metal content. Secondary heavy metal pollution occurs due to dissolution from treatment sludge from where heavy metals can be mobilized again and access into the drinking water and food chain. Chemical or biological means are inadequate for removal of heavy metals reaching the food chain and thus, they accumulate within the body [20].

Environmental Cr (VI) contamination is an increasing concern due to its global spreading in high concentrations in water and soil by natural and anthropogenic activities. The release of chromium, which is widely used in industry, into the environment causes major contamination in soil and water. After chromium is released into the environment, it exists in the most stable forms of Cr (III) and Cr (VI). Cr (III) is less toxic than Cr (VI) and is used by the human body [21]. Meanwhile, Cr (VI) is highly toxic, causing problems such as diarrhea, vomiting, and carcinogenic effects in the lungs and kidneys [22, 23] Furthermore, the International Agency for Research on Cancer has classified Cr (VI) as a carcinogenic chemical in the first group [24].

2. GENERAL INFORMATION

2.1. Chromium

In the crust of the earth, chromium is an element that is found in relatively high concentrations. Although chromium has a wide range of oxidation states, from -2 to +6, only the 0, +3, and +6 states are stable in environmental conditions [25]. Chromium was discovered by Nicholas Vauqueilin in 1978 and it is a gray, shiny and brittle metal. Chromium has a wide range of uses due to its hardness, corrosion resistance and magnetic properties. It is used in the production of stainless steel together with nickel because it has corrosion resistance and prevents discoloration in the steel [26].

Hexavalent chromium Cr (VI) is mostly present as dichromate ($Cr_2O_7^{-2}$) and chromate ($CrO4^{-2}$) ionic forms in aqueous solutions. Depending on the solution pH, Cr (VI) can be found in water as chromate ($CrO4^{-2}$), dichromate ($Cr_2O_7^{-2}$), hydrogen chromate ($HCrO_4^-$) and chromic acid (H_2CrO_4).

The mining and metalworking industries, leather manufacturing, paint production, wood and paper production, and dyeing are increasing the chromium concentration in wastewater. Furthermore, the ash fallout from the combustion of coal or urban waste for electricity generation and the manufacturing of second-generation fertilizers result in a higher Cr (VI) concentration in soil and water. National discharge restrictions for chromium in water differ depending on the kind of industry or aquatic environment receiving the effluent. The national discharge limitations for water for the majority of European countries have been recently reviewed by Tumolo et al. (2020). The discharge limitation listed in Table 2.1 varies according to the type of industry, the regional regulation, and the kind of aquatic environment that is receiving the discharge [27].

Table 2. 1. Discharge limitations for total Cr (total) and Cr (VI) into water bodies at the national scale (values are given as milligrams per liter) [27]

Country	France	Germany	Hungary	Italy	The Netherlands	Spain
Cr^{Total}	0.5	0.1–0.5	0.2–1	2–4	0.5	5
Cr^{6+}	0.1	0.05–0.5	0.1–0.5	0.2	0.1–2	0.3

In Turkey, the wastewater generated as a result of the applications of the petroleum, textile, mining, paint and metal industries, especially the leather industry, contains toxic Cr (VI) ions. Table 2.2. lists the limitation of Cr (VI) discharge from several industries in Turkey.

Table 2. 2. Chromium discharge standards of waste water from various industries to the receiving aquatic environment in Turkey [15]

Industry	Mining	Oil	Leather	Paint	Petro-chemical	Metal
Cr (VI) Concentration (mg/L)	0.3	0.5	0.5	0.5	0.5	0.5

The pollutants present in industrial waste water must be eliminated before being released to the environment so as not to degrade water quality.

2.2. Wastewater Treatment Methods

Wastewater treatment covers all the physical, chemical and/or biological remediation procedures applied for the recovery some or all of the physical, chemical and microbiological features of wastewater produced as a result of numerous uses. The treatment also aims for sustaining the natural properties of the receiving environment to which wastewater is discharged [15].

Heavy metals are toxic to living organisms and should be removed from water and wastewater. Frequently applied techniques include chemical precipitation, membrane filtration, ion exchange, and adsorption for the remediation of heavy metal bearing aqueous solutions [28].

2.2.1. Chemical precipitation

It is possible to convert heavy metal ions into insoluble solid particles using chemical precipitation method. Sedimentation or filtration can be used to seperate the precipitated particles. There is a strong correlation between pH and the efficiency of heavy metal removal, thus, pH adjustment is a critical step in chemical precipitation. Once pH has been adjusted, the agent reacts with the soluble metal ions, and converts them into the insoluble solid. Basic pH conditions (pH > 7) are often preferred for the recovery of heavy

metals such as Zn^{2+}, Cd^{2+}, Cr^{3+}, Pb^{2+}, Hg^{2+} or Ni^{2+} [29]. In order for some components to be precipitated directly, they must first be reduced or oxidized to a valence state [30]. Salts including OH^-, S^{2-}, CO_3^{2-}, PO_4^{3-} groups are commonly employed for heavy metals [31, 32].

Chemical precipitation requires that considerable amounts of chemicals are used for the reduction of metal ions to an allowable level for discharge. These chemicals are a major contributor to potential pollution, and large amounts of toxic sludge are formed as a result of the precipitation processes [33].

2.2.2. Membrane filtration

Membrane processes have an important place in separation technologies. The main membrane processes are hemodialysis/hemofiltration, reverse osmosis, ultra filtration, micro filtration and electrodialysis [34]. In electrodialysis, a selectively permeable membrane is used for the transportation of ions. The driving force of this process is the electropotential difference. Membranes can have anion or cation selectivity, depending on the membrane type, positive or negative ions pass through the membrane [35]. Microfiltration and nanofiltration are based on the principle of hydrostatic pressure difference, while reverse osmosis is based on the principle of mass transfer [28]. Membrane processes have a major drawback due to the expensive membrane materials required [36].

2.2.3. Ion exchange

The principle of ion exchange process is the reversible exchange of ions from the solid to the liquid phase [30]. The metal ions in the solution are removed using a cation or anion containing ion exchanger. Widely used ion exchange resins made from synthetic organic materials. This technique requires low-concentration metal solutions and is pH-sensitive. The purpose of ion exchange resins is to remove either positive or negative-charged ions from an electrolyte solution and replace them with an equal amount of the oppositely charged ions [37]. Reduced ion exchange capability upon regeneration and the high cost of synthetic ion exchangers make this technique impractical in many situations.

2.2.4. Adsorption

Adsorption refers to the mass transfer process in which a material present in the liquid phase is transported to the solid surface and is bonded either by chemical and/or physical interactions. Adsorbate is the material that adheres to a surface, and adsorbent is the material that adsorbs. Adsorbents may be in solid or liquid forms, and of natural or synthetic origin. Recently, cost efficient adsorbents made from agricultural residues, industrial by-products, several natural substances and or modified biopolymers with various compositions have been used to eliminate heavy metals from contaminated wastewater. Technical applicability and cost-effectiveness are critical criteria in selecting the best adsorbent for treating inorganic wastewater [38]. The adsorption process is examined in 3 groups according to adsorbent-adsorbate interactions: physical adsorption, chemical adsorption and exchange adsorption.

2.2.4.1. Physical adsorption

The type of adsorption that takes place as a result of Van der Waals attraction forces between the solid surface and the molecules of the adsorbed substance is defined as physical adsorption. In this case, the adsorption is multilayered and regeneration is easy. The adsorption equilibrium is a double-sided reaction. The process of physical adsorption is reversible, and it is possible to desorb molecules that have been adsorbed onto an adsorbent surface. Since electrostatic forces mediate physical adsorption, no additional activation energy is required for adsorption to take place. While the process of physical adsorption is mostly exothermic, the rate of adsorption slows rapidly as the temperature rises [39, 40].

2.2.4.2. Chemical adsorption

In chemical adsorption, chemical bond formation takes place between the adsorbed substance and the solid adsorbent surface. Chemical adsorption is irreversible and monolayer and usually occurs at high temperatures and it is also difficult to regenerate. Generally, the energy required for adsorption of one mole of molecules is close to the energy required for chemical bond formation [19].

2.2.4.3. Exchange adsorption

Exchange adsorption, which is generally known as ionic adsorption, occurs due to the electrical attractive forces between the adsorbate-adsorbent pair. With the effect of electrostatic attraction forces, the ions are attached to the charged areas on the surface. In exchange adsorption, the adsorbent and adsorbate have equal and opposite charges. Ion charges and the pore structure of the adsorbent are important parameters affecting the adsorption [41].

Most usually, the adsorption process can not be elucidated with only one of the adsorption types summarized above. In many adsorption processes, different adsorption types can be seen together or sequentially [42].

In comparison to other common techniques (such as membrane filtration or ion exchange), adsorption has a number of significant beneficial issues, including ease of operation, the presence of low cost efficient adsorbents, and feasibility. These advantages are highly important in terms of economical and environmental aspects.

2.2.5. Adsorbents used in study

2.2.5.1. Chitosan

Chitin, a natural polymer which can be found in crustacean shells including shrimp, crabs, insects, and so on, is the second most frequent polymer after cellulose [43]. Chitosan is a polyaminosaccharide formed by the deacetylation of chitin. Chitosan is preferred as an adsorbent for heavy metal or dye removal from wastewaters owing to its special traits such as non-toxicity and availability of different functional groups for adsorption. $(C_6H_{11}O_4)_n$ is the chemical formula of chitosan [44].

Chitosan contains $-NH_2$ and -OH groups that can function as active sites for adsorption of pollutants. Different strategies such as cross-linking, chemical modification or blending with different polymers can be used to improve the chemical and mechanical strength of chitosan. In this context, polyvinyl alcohol is one of the most preferred polymers for the modification process due to its high biocompatibility, hydrophilic nature, superior mechanical strength and flexibility, thermal stability and non-toxicity, easy availability and low cost [45].

2.2.5.2. Polyvinyl alcohol

Polyvinyl alcohol (PVA) is a colorless and thermoplastic polymer which is soluble in water. It is formulated with $(C_2H_4O)n$ and obtained by hydrolysis of polyvinyl acetate. Thanks to the excellent properties and easy modification ability of PVA, it is used for wastewater treatment. CS/PVA blends have good durability due to their unique intermolecular interactions each other [46].

2.3. Working Principle of Fixed-Bed Adsorption Column

Up to date, a number of different column working principles have been developed such as the pulsed-bed, fixed-bed, continuous fluidized-bed and moving bed columns which have been proven to be promising for water treatment. There are benefits and drawbacks of each adsorption method. Due to its effectiveness and ability to adapt, fixed-bed column adsorption is the technique of choice for industrial water purification [46].

Adsorption in a fixed-bed continuous flow column may be considered as a kind of dynamic adsorption due to the fact that the influent, which is the pollutant solution, continually enters and exits the column.

The kinetic column parameters and breakthrough curves (BCs) are determined by the fixed bed column adsorption data, which also helps to define the adsorbent's performance and explain the interaction of the adsorbent with the adsorbate.

The notion of the BC is useful for the establishment of the efficacy of a fixed-bed adsorption column [47]. Adsorption column process design is dependent on several factors, including breakthrough time and BC shape. Column operating factors including C_0, Q, and h_{bed} affect the shape and characteristics of the BC. These characteristics must be experimentally determined to assess column effectiveness and scale up. Normalized concentration identified as the ratio C_t to C_0 with respect to time or effluent volume is used to depict BCs [48].

Typically, the effluent concentration as a function of operating time or throughput volume is used to explain the behavior of fixed-bed dynamic systems [49]. The mass transfer zone (MTZ), BC and typical concentration profiles in a fixed bed column are given in Figure 2.1. As seen in Figure 2.1, in the adsorption process in the fixed bed, mass transfer initially

takes place at the entrance of the bed and near the entrance. As the MTZ shifts from the column inlet to the exit, the metal concentration at the column exit gradually increases over time. The column continues to operate until C_t and C_0 are equal [50]. As seen in Figure 2.1, the BC is formed by processing the C_t/C_0 values with respect to time or the volume of water passing through the column. The BC normally takes the form of an 'S'.

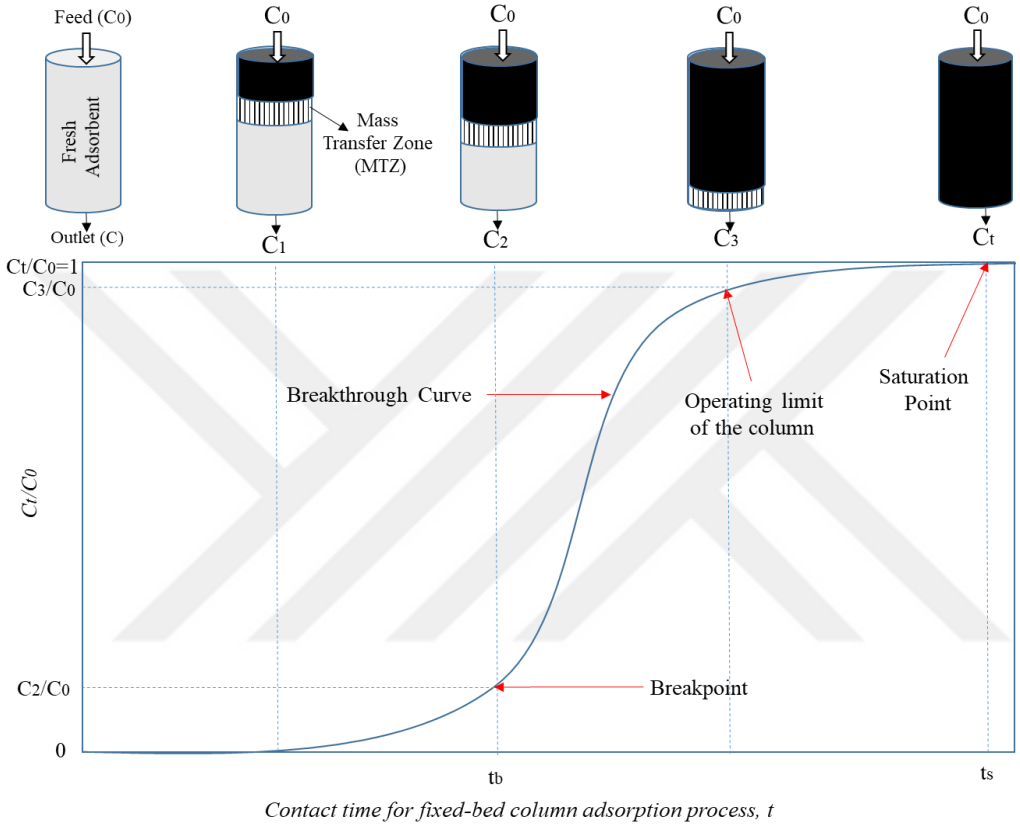

Figure 2. 1. A schematic representation of a typical BC for a fixed-bed adsorption method

The efficacy of adsorption in fixed bed columns is explained via BC expression. In order to construct the BC in a fixed bed column, the exit-to-initial concentration ratio (C_t/C_0) must be determined in relation to time or the volume of effluent. Output volume (V_{eff}) is determined using Equation 2.1.

$$V_{eff} = Q.t_{tot} \quad (2.1)$$

The t_{tot} and Q represents to total flow time (min) and volumetric flow rate (ml/min), respectively.

A BC is obtained by plotting the concentration adsorbed, (C_{ad}; mg/L) against t. The area under this curve (A) gives the total adsorbate amount (maximum capacity of the column). For the given C_0 and Q, the total amount of adsorbate (q_{tot}) adsorbed in the column is calculated with the help of Equation 2.2 .

$$q_{tot} = \frac{QA}{1000} = \frac{Q}{1000} \int_{t=0}^{t_{tot}} C_{ad}\,dt \tag{2.2}$$

The total quantity of Cr (VI) entering the column, (m_{tot}; g) can be determined by using equation 2.3.

$$m_{tot} = \frac{C_0 Q t_{tot}}{1000} \tag{2.3}$$

Equation 2.4 can be used to determine the equilibrium Cr (VI) uptake capacity of the column, q_e (mg/g).

$$q_e = \frac{q_{tot}}{m} \tag{2.4}$$

Hereby, ‘m’ symbolyzes the quantity of adsorbent in the bed (g). The entire amount of Cr (VI) adsorbed (q_{tot}) to the entire amount of Cr (VI) sent to the column (m_{tot}) ratio can be utilized to find the Cr (VI) removal percentage (R%) (Eqn. 2.5) [48].

$$R\% = \frac{q_{tot}}{m_{tot}} \times 100 \tag{2.5}$$

2.4. Mathematical Models

Appropriate models need to be used to describe process mechanisms, explain and analyze experimental data, and predict optimum process and changing experimental conditions. The following kinetic models have been developed to precisely describe the adsorption dynamics of fixed bed columns.

2.4.1. Thomas model

The plug flow behavior of the fixed bed can be clarified by the Thomas model. It adheres to the principles of the second-order reversible reaction dynamics and relies on the Langmuir isotherm for systems that are in equilibrium. [51]. The linearized version of the model is explained below (Eqn. 2.6).

$$\ln\left(\frac{C_t}{C_0}-1\right)=\frac{k_{Th}q_0m}{Q}-\frac{k_{Th}C_0V_{eff}}{Q} \tag{2.6}$$

k_{Th} and q_0 values can be evaluated from the slope and intercepts of the line obtained from the graph of $\ln[(C_0/C_t)-1]$ versus time under different experimental conditions.

2.3.2. Adams-Bohart model

Adams and Bohart developed a basic equation which defines the interaction between C_t/C_0 and t in a column system for Cl_2 adsorption on charcoal relied on the surface reaction theory. It claims that equilibrium does not occur instantaneously; thus, the adsorption rate is proportionate to both the adsorption capacity and the adsorbate concentration. The initial section of the BC is described using the Adams-Bohart model [53, 54]. The model is written in Eqn. 2.7.

$$\ln\left(\frac{C_t}{C_0}\right)=k_{AB}C_0t-k_{AB}N_0\frac{z}{U_0} \tag{2.7}$$

Using equation 2.7, N_0 values can be found from the intercept of the line drawn between $\ln (C_t/C_0)$ and t, and k_{AB} from its slope. This equation is applied for the $C_t < 0.5C_0$ section of the curve.

2.3.3. Yoon-Nelson model

Yoon and Nelson's studies resulted in the development of a simplified model for the adsorption of gases on activated charcoal and the behavior of BCs. This model declares that the rate of decrease in concentration for each adsorbate molecule in the adsorption system is proportional to the rate of its adsorption [52].

The linear Yoon-Nelson model equation for the one-component system is given in Eqn 2.8.

$$\ln\left(\frac{C_t}{C_0 - C_t}\right) = k_{YN}t - k_{YN}\tau \tag{2.8}$$

By plotting ln $[(C_t/(C_0-C_t))]$ vs. time, τ is found from the intersection point of the line and k_{YN} is found from its slope.

2.3.4. BDST model

The BDST model, a modified version of the Adams-Bohart model, is utilized for the determination of the column uptake capacity [55]. This model assumes that parameters such as intraparticle diffusion and external mass transfer resistance can be neglected. Adsorption dynamics is regulated by a surface chemical reaction between the adsorbate and the adsorbent [56]. Equation of the model can be expressed as Eqn. 2.9.

$$t = \frac{N_0 Z}{C_0 u} - \frac{1}{k_{BDST} C_0} \ln\left(\frac{C_0}{C_t} - 1\right) \tag{2.9}$$

N_0 and k_{BDST} values can be found from the slope and intercept of the line drawn between the h_{bed} (Z) and the service time (t). The simplified version of the BDST model is as follows:

$$t = aZ\text{-}b \tag{2.10}$$

$$a = \frac{N_0}{C_0 u} \tag{2.11}$$

$$b = \frac{1}{k_{BDST} C_0} \ln\left(\frac{C_0}{C_t}\text{-}1\right) \tag{2.12}$$

The slope constant for a variable flow rate can be determined by using the Eqn. 2.13.

$$a' = a\frac{Q}{Q'} \tag{2.13}$$

Where a and Q represent the previous slope and flow rate, and a' and Q' represent the new slope and flow rate, respectively.

For different initial concentrations, the following equations provide the new slope and new intercept.

$$a' = a\frac{C_o}{C_o'} \tag{2.14}$$

$$b' = b\frac{C_o}{C_o'}\ \ln\left(\frac{\frac{C_0'}{C_t'} - 1}{\frac{C_0}{C_t} - 1}\right) \tag{2.15}$$

Where b' and b are the new and old intercepts and C_0' and C_t' are the new inlet and outlet concentrations at time t, respectively.

When the service time is equal to zero, the following equation may be used to get the critical bed depth (Z_0), which is the theoretical depth of adsorbent that must be present in order to prevent the adsorbate concentration from being greater than C_t at the time t=0:

$$Z_o = \left(\frac{u}{N_0 k_{BDST}}\right) \ln\left(\frac{C_0}{C_t} - 1\right) \tag{2.16}$$

3. MATERIAL AND METHOD

3.1. Materials

3.1.1. Chemicals

A list of the major chemicals used in this study is provided in Table 3.1 along with their sources and purities.

Table 3. 1. The chemicals used in the study

Chemical Name	Source
Sodium hydroxide, reagent grade ≥ 98%	Sigma-Aldrich
Hydrochloric acid, reagent grade 36.5-38 %, 12 M	
Sulfuric acid, reagent grade 96-97 %, 18 M	
Diphenyl carbazide, reagent grade	
Acetone, reagent grade ≥ 99%	
Polyvinyl alcohol, MW: 31000-50000, 99% hydrolyze	
Potassium chromate	Merck, Germany
Chitosan, MW: 100000-300000, 85% deacetylation degree	Acros, Belgium

3.1.2. Instruments

- UV-Vis spectroscopy, Cary Win 2.0
- Stove, Binder
- pH meter, Wtw Inolab Ph 7110
- Peristaltic pump, BTF Fluid
- Hotplate stirrer, Velp Scientifica
- Analytical Balance, Mettler Toledo AG286

3.1.3. Solutions

Cr (VI) Stock Solution: Cr (VI) stock solution was prepared with 3.73 g K_2CrO_4 (potassium dichromate) dissolved in extra pure water to make 1000 ppm solution. During the experiments, the desired concentrations were attained by dilution of the stock solution.

Sodium Hydroxide Solution: In order to adjust the pH, 1 N solution of sodium hydroxide (NaOH) was used. To make the solution, 40 g of NaOH was dissolved in an adequate quantity of pure water.

Sulfuric Acid Solution: 0.2 M H_2SO_4 (sulfuric acid) solution was used for pH adjustment. 11.1 mL of 96% sulfuric acid solution (18 M) was dissolved in distilled water.

***Diphenyl Carbazide Solution*:** After weighing 0.5 g of diphenyl carbazide, it was dissolved in 100 ml of acetone. Since the solution can be affected by light and deteriorated, it was stored in amber glasses.

Acetic Acid Solution: In order to prepare a 4% solution by volume, 20 ml of acetic acid was transferred into a 500 ml flask and filled with distilled water.

Chitosan Solution: To prepare a 4% chitosan solution, 4 g of chitosan was weighed into a 100 ml flask and filled with 4% acetic acid solution.

Polyvinyl Alcohol solution: A water bath at 80 °C was prepared. To prepare 10% PVA solution, required amount of PVA was weighed and dissolved in distilled water by stirring in the water bath.

3.2. Method

3.2.1. Synthesis of H-CS/PVA adsorbents

In this study, H-CS/PVA blend beads were selected as adsorbents for Cr (VI) removal. For the synthesis of blend beads firstly, chitosan (4% wt.) and polyvinyl alcohol (10% wt.) solutions were prepared. Then, they were mixed in equal volumetric ratio and this mixture was transferred into 1 M NaOH bath with the help of a pump-syringe system, and hydrogel formation was expected. Afterwards, the hydrogels were washed with ultrapure water for removal of excess NaOH from the structure and to neutralize the pH.

After rigorous washing, the hydrogels were taken into a stainless steel autoclave (300 ml) and subjected to thermal treatment at a predetermined temperature and time (140 ˚C, 12 hours) [11]. As the last stage of the synthesis step, corresponding to the end of thermal treatment, the carbonized beads were removed from the autoclave and left to dry at room temperature.

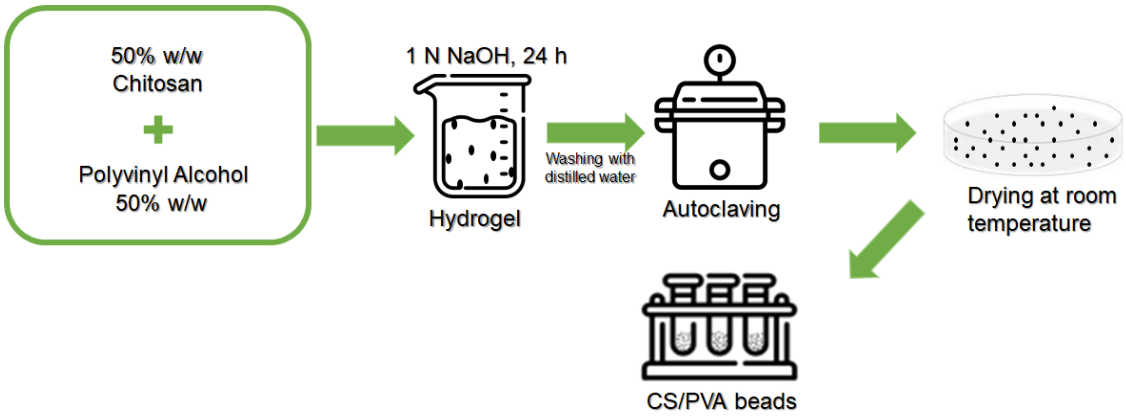

Figure 3. 1. Sythesis of H-CS/PVA adsorbents

3.2.2. Characterization methods

The structural, morphological and physicochemical characteristics of H-CS/PVA adsorbents were investigated prior to and afterwards the Cr (VI) adsorption process by the help of a number of different characterization techniques, including SEM, SEM-EDX, FTIR and BET.

3.2.2.1. SEM and SEM-EDX analysis

SEM is a preferred instrument for examining and analyzing micro- and nanoscale imagery characterization of solid materials. SEM employs a focused beam of electrons on the sample surface to generate signals. Signals derived from sample-electron interactions provide information about the morphological properties of the anayzed sample such as surface morphology and infra-structure [56].

EDX spectroscopy is utilized to determine the chemical content of a material using a scanning electron microscope. Material evaluation and identification, as well as contamination detection, are examples of EDX applications [57].

SEM and SEM-EDX analyses were realized at various magnifications within the range 150x-10000x by using an FEI Quanta Feg 250 instrument in the NABILTEM Research Laboratory at Namık Kemal University.

3.2.2.2. FTIR analysis

In order to identify functional groups in absorbent materials, FTIR spectroscopy is a widespread analytical method [58]. In FTIR spectroscopy, some IR radiations are absorbed by the sample, while others pass through the sample (transmitted). Each bond present in the molecule vibrates at a different energy and thus absorb different wavelengths of infrared radiation. The characteristic fingerprint of a molecule is composed of these individual absorption bands, each with a different frequency and intensity [59].

The FTIR analysis of pre-adsorption and saturated H-CS/PVA adsorbents was carried out at the Namık Kemal University Research Laboratory (NABILTEM) by using a Bruker Vertex 70 ATR spectrometer within the range of 500-4000 cm^{-1} with 4 cm^{-1} resolution.

3.2.2.3. BET analysis

BET theory clarifies the physical absorption of gas molecules on a solid surface and this technique is used to determine the specific surface area and the pore volume. BET testing typically uses nitrogen as a gaseous adsorbate. Nitrogen is the most commonly used gas adsorbate for surface probing in BET analysis [60].

The BET analysis was performed at Yıldız Technical University Central Laboratory (BITUAM) utilizing a Quantachrome NovaWin2 instrument. Before being analyzed, the samples were degassed for 8 hours at 80˚C.

3.2.3. Adsorption column studies

Cr (VI) removal was fulfilled in a fixed bed column. The experimental configuration comprised of a column including a bed filled with hydrothermally treated CS/PVA beads, a peristaltic pump, a feed solution tank and a receiver tank for the effluent stream. An 2.5 cm inner diameter, cylindrical glass column with Teflon tap was used to install the continuous flow column. Figure 3.2 shows the experimental configuration used for adsorption in the fixed bed column.

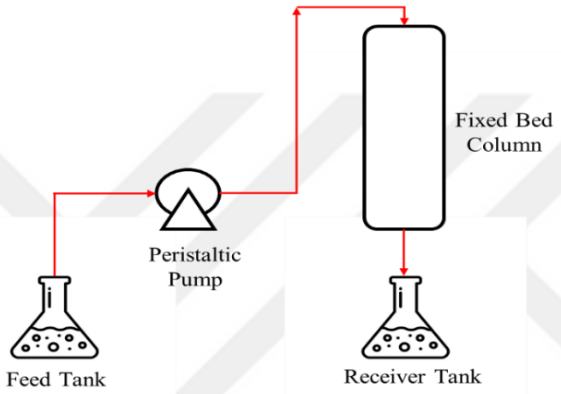

Figure 3. 2. Experimental configuration of the continous flow column for Cr (VI) adsorption

The Cr (VI) concentration of the effluent was monitored during the experiments by taking samples at predetermined time intervals. Experiments were performed at different Q, h_{bed}, and C_0 conditions. In any case, experiments were continued until C_t was equal to C_0.

The concentration of Cr (VI) was determined via colorimetric analysis. using diphenyl carbazide reagent. For this purpose, after adding 2 mL of diphenyl carbazide to 1 ml sample taken from the Cr (VI) solution adjusted to pH 3 by the help of 0.2 N H_2SO_4 solution, it was filled to 50 milliliters with distilled water. Cr (VI) reacted with diphenylcarbazide to form a red-violet colored compound. After 5-10 minutes the color formation was observed, the analysis was carried out in a UV Spectrophotometer at a wavelength of 540 nm. Afterwards calibraton curve, which related absorbance and concentration, was drawn (Appendix A). The Cr (VI) concentration of solution was then calculated by the help of the absorbance value and the calibration curve.

Also in adsorption studies, Cr (VI) was determined with UV spectroscopy by taking samples from the effluent of column at certain time intervals.

3.2.3.1. Investigation of effect of flow rate on Cr (VI) removal

The effects of Q on Cr (VI) removal in a continuously operated column filled with H-CS/PVA were investigated by keeping C_0 and h_{bed} constant at 20 mg/L and 2 cm, respectively. Q was set either to 2.5, 5 or 7.5 mL/min in experiments.

3.2.3.2. Investigation of effect of initial solution concentration on Cr (VI) removal

The effects of C_0 on Cr (VI) removal in a continuously operated column filled with H-CS/PVA were investigated by keeping Q and h_{bed} constant at 2.5 mL/min and 2 cm, respectively. C_0 was set either to 20, 40 or 60 mg/L in experiments.

3.2.3.3. Investigation of effect of bed height on Cr (VI) removal

The effects of h_{bed} on Cr (VI) removal in a continuously operated column filled with H-CS/PVA were investigated by keeping the the Q and C_0 constant at 5 mL/min and 40 mg/L, respectively. h_{bed} was set either to 2, 4 or 6 cm in experiments.

3.2.4. Mathematical Model Studies on Fixed Bed Column Data

Thomas, Adams-Bohart, Yoon-Nelson and BDST models were employed to explain the adsorption mechanism and it was determined which model was more suitable.

As explained in section 2.3 model constants for each studied model were estimated using linear and non-linear regression techniques to adsorption data. The data were used to construct plots of ln $((C_0/C_t)-1)$, ln $(C_t/(C_0-C_t))$, and ln $(C_0/C_t - 1)$ versus time for evaluation the parameters of each model.

3.2.5. Error functions

To determine the most appropriate kinetic model, error analysis was carried out. Calculating the difference between the experimental results and the values determined from the applied model, the magnitude of error was calculated for each data point.

Nonlinear Chi-square Test (X^2), Average Relative Error (ARE) and Marquardt's Percent Standard Deviation (MPSD) equations were involved for error calculations. The equations are provided below in respective order (Eqs. 3.1- 3.3).

$$X^2 = \sum_{i=1}^{n} \frac{(q_{e,\,meas} - q_{e,\,calc})^2}{q_{e,\,meas}} \tag{3.1}$$

$$ARE = \frac{100}{n} \sum_{i=1}^{n} \left| \frac{q_{e,\,meas} - q_{e,\,calc}}{q_{e,\,meas}} \right| \tag{3.2}$$

$$MPSD = 100 \sqrt{\frac{1}{n-p} \sum_{i=1}^{n} \left(\frac{q_{e,\,meas} - q_{e,\,calc}}{q_{e,\,meas}} \right)^2} \tag{3.3}$$

In these equations, q_{meas} and q_{calc} are values measured in experimental study and evaluated from the model, respectively, and 'n' is the number of data points. The appropriate model was determined by considering the lowest error values (X^2, ARE, MPSD). Excel Solver program was utilized for performing error analysis.

4. RESULTS AND DISCUSSION

H-CS/PVA blend beads synthesis achieved in the laboratory. Each step of synthesis is given in Figure 4.1.

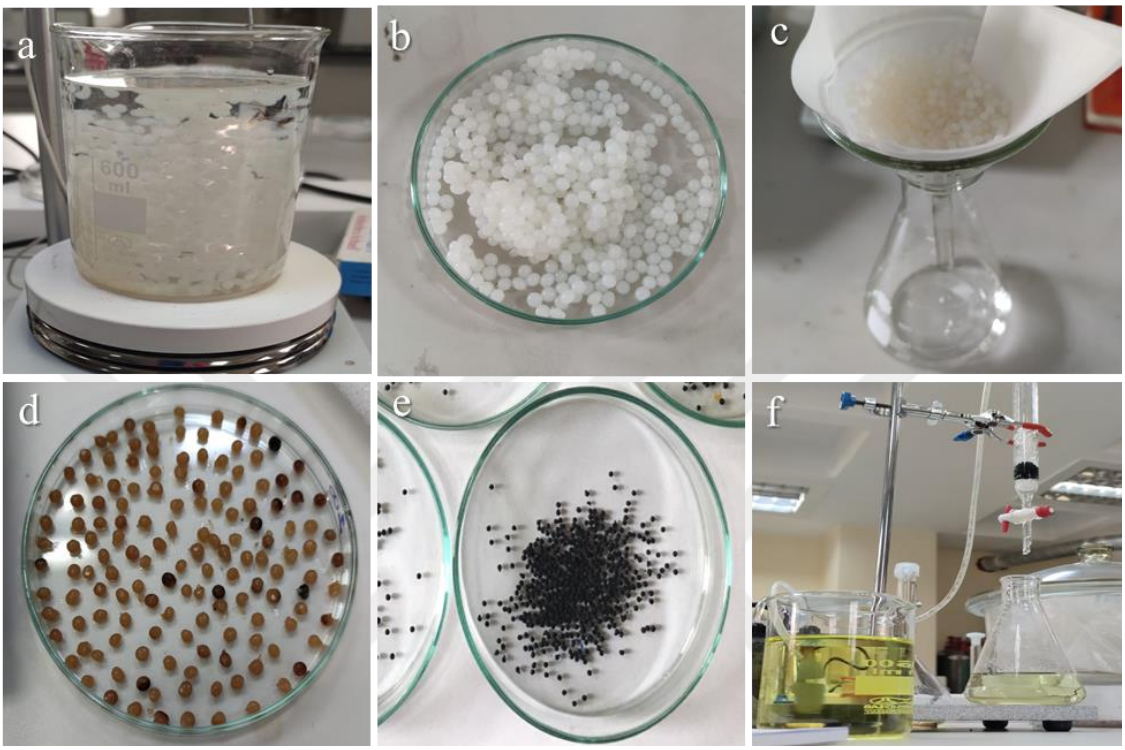

Figure 4. 1. Steps of H-CS/PVA bead synthesis

It can be seen from the Fig. 4.1.a, after the chitosan solution was prepared, hydrogels were formed by transferring the solution into NaOH bath. In the next step, the hydrogels were washed with extra-pure water to clean off the NaOH and the pH was neutralized. Neutral hydrogels were autoclaved and exposed to hydrothermal treatment (140˚C, 12 h). After this period, the carbonized beads removed from the autoclave were left to dry at room conditions. Adsorption experiments were performed using the fixed-bed colum working approach as shown in Fig. 4.1.f., a glass column was filled with the desired amount of H-CS/PVA beads which were supported by cotton wool layers to achieve a specific bed depth and to prevent adsorbent loss throughout solution flow. The adsorption capacity of H-CS/PVA beads was determined experimentally by applying different column parameters.

The following parts will provide an in-depth explanation of the impacts of process parameters on the adsorption efficiency. Column capacity and column performance were determined for each system by using the obtained BCs. By applying Thomas, Yoon-Nelson, Adams-Bohart and and BDST models to the experimental BC data, it was investigated which model could best predict the BCs and the kinetic constants of these models were calculated.

4.1. Effects of Parameters on Column Study

4.1.1. Flow rate effects on Cr (VI) removal

The flow rate (Q) is one of the most significant factors when evaluating the effectiveness of a fixed-bed column. Q was adjusted to either 2.5, 5 or 7.5 ml/min while keeping the h_{bed} and C_0 at 2 cm and 20 ppm, respectively. The BCs plotted using column data is shown in Fig. 4.2.

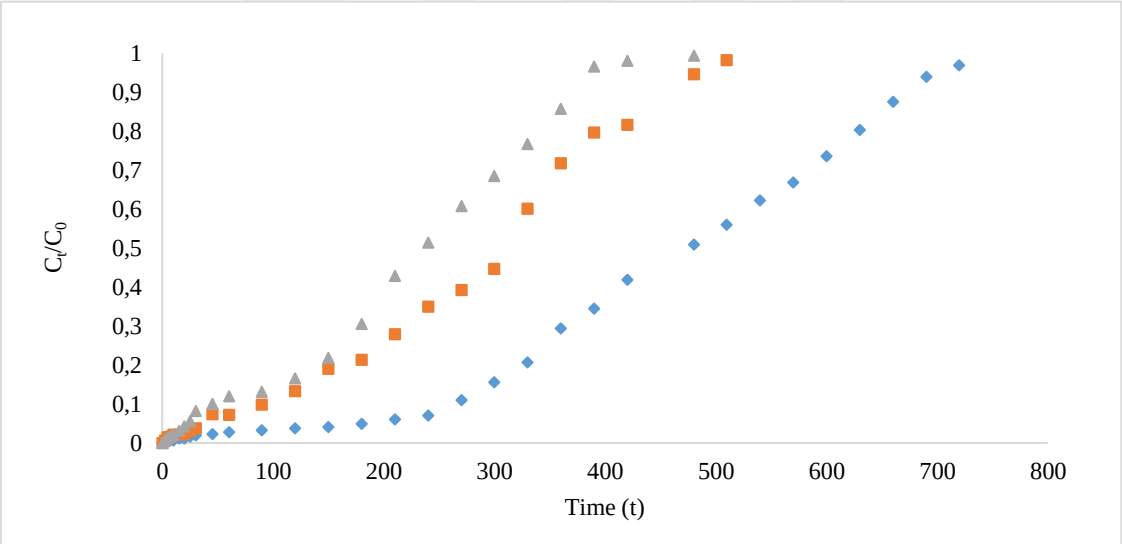

Figure 4. 2. BCs at different flow rates at C_0 = 20 ppm, h_{bed} = 2 cm (Blue, orange and gray represent Q; 2.5, 5, 7.5 ml/min respectively)

The trends in Fig. 4.2 show that breakthrough time decreased when Q increased. Therefore, the curve get steeper. The residence time of chromium ions in the column is reduced in the order of increasing Q. Therefore, the adsorption of chromium ions onto H-CS/PVA beads were limited for higher Q value. Table 4.1 shows the fixed-bed column parameters for Cr (VI) removal at various flow rates.

Table 4. 1. Fixed-bed column parameters for different flow rates

C_o (mg/l)	Q (ml/min)	h_{bed} (cm)	t_b (min)	t_{sat} (min)	m_{tot} (mg)	q_{tot} (mg)	q_e (mg/g)	V_{eff} (ml)	% Removal
20	2.5	2	250	720	36	23.12	5.36	1800	64.2
20	5	2	60	510	51	22.62	5.24	2550	44.36
20	7.5	2	40	480	72	16.64	3.85	3600	23.12

According to the values shown in Table 4.1. significant decreases were recorded in the saturation and breakthrough time since the Q increased. This result was most probably because of the prolonged MTZ and decreased diffusion coefficient [57]. Similar phenomena has been noticed in the removal percentage of chromium ions. The insufficient contact time for metal ions to move into the pores of the H-CS/PVA beads results in a low of removal efficiency. Thus, leaving the column prior to attainment of equilibrium. Furthermore, decreases are anticipated in film thickness for the external mass transfer and in the MTZ as Q increases. These findings implied that low volumetric flow rates were in favor of removal of chromium. Other researchers have also made similar observations [54, 56, 58].

4.1.2. Initial solution concentration effects on Cr (VI) removal

For the purpose of evaluation of C_0 effect on the removal of Cr (VI) ion with H-CS/PVA in a fixed bed, experiments were conducted at constant h_{bed} and Q of 2 cm and 2.5 ml/min, respectively. Figure 4.3 shows influent Cr (VI) concentration effect (20, 40 and 60 mg/l) on BCs.

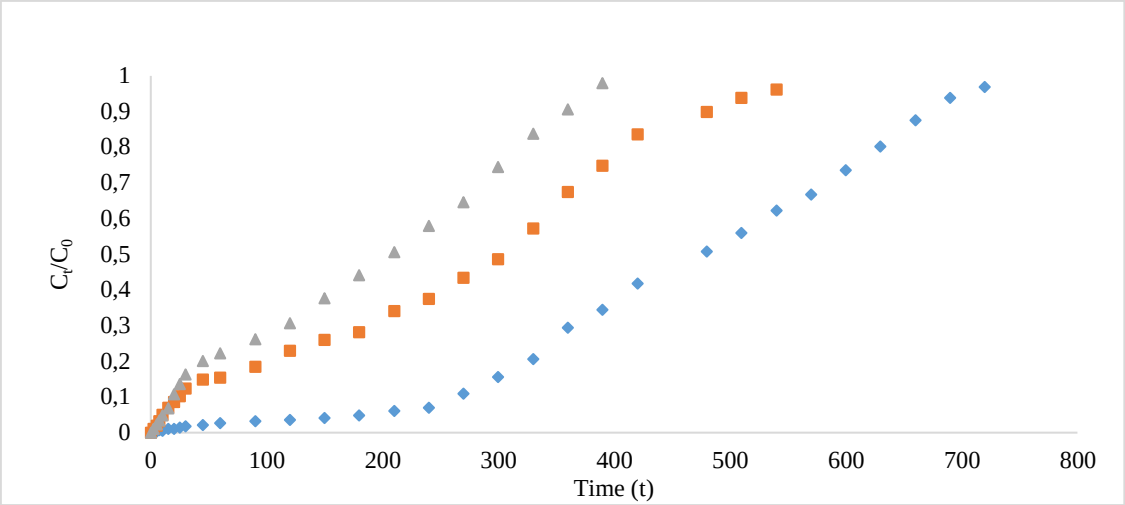

Figure 4. 3. BCs at different initial concentrations at Q=2,5 ml/min, h_{bed} = 2 cm (Blue, orange and gray represent C_0; 20, 40 and 60 ppm respectively)

Figure 4.3 shows that the BCs moved left and breakthrough times dropped from 250 to 20 min when the input concentration increased from 20 to 60 ppm. At higher chromium amounts in the influent, accessible absorbent sites are rapidly filled thanks to the higher driving force for mass transfer of chromium ions, resulting in a shorter breakthrough time. The sharpness of the BCs increased as a result of increased influent concentration. Adsorption of Cr (VI) onto H-CS/PVA beads has been demonstrated to be driven by intraparticle diffusion [55, 59, 60].

Table 4. 2. Fixed-bed column parameters for different C_0

C_o (mg/l)	Q (ml/min)	h_{bed} (cm)	t_b (min)	t_{sat} (min)	m_{tot} (mg)	q_{tot} (mg)	q_e (mg/g)	V_{eff} (ml)	% Removal
20	2,5	2	250	720	36	23.12	5.35	1800	64.2
40	2,5	2	25	540	54	27.94	6.47	1350	51.75
60	2,5	2	20	390	58.5	35.14	8.11	975	60.06

According to the values listed in Table 4.2, the enhancement in adsorption capacity was accompanied by an increase in C_0. This can be clarified in view of the mass transfer which was fastened by a higher concentration gradient in the order of increasing C_0. Also the findings match with the results of other research works [55, 58-60].

4.1.3. Bed height effects on Cr (VI) removal

In a fixed-bed column, the total amount of chromium taken up depends on how much adsorbent is inside the column. Figure 4.4 shows how the bed heights of 2, 4 and 6 cm effect the BCs with a constant Q of 5 mL/min and an influent concentration of 40 ppm.

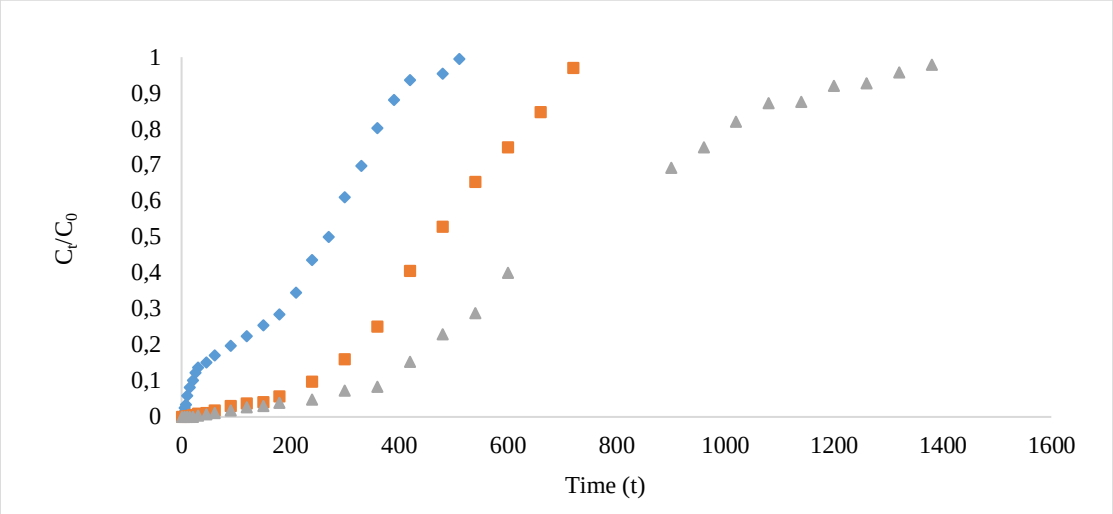

Figure 4. 4. BCs at different bed heights (Q=5 mL/min, C_0=40 ppm) (Blue, orange and gray represent hbed; 2, 4 and 6 cm respectively)

As seen in Fig. 4.4, a decrease in h_{bed} resulted in steeper BCs. At low h_{bed}, axial dispersion dominates the mass transfer and prevents diffusion [61]. Breakthrough time was shortened from 240 to 45 min at corresponding h_{bed} of 6, 4 and 2 cm. Increasing the bed height leads to widened the MTZ [58].

Table 4. 3. Column parameters for different bed heights

C_o (mg/l)	Q (ml/min)	h_{bed} (cm)	t_b (min)	t_{sat} (min)	m_{tot} (mg)	q_{tot} (mg)	q_e (mg/g)	V_{eff} (ml)	% Removal
40	5	2	45	510	102	42.92	9.95	2550	49.98
40	5	4	180	720	144	76.67	10.81	3600	53.24
40	5	6	240	1380	276	155.86	15.53	6900	56.47

The findings from Table 4.3. showed that increasing h_{bed} from 2 cm to 6 cm increased percentage chromium removal thanks to increasing of the adsorbent amount and more adsorption sites were accesible. Likewise, solution residence time in the column increased since the h_{bed} increased, permitting the chromium ions to diffuse deeper into the beads. In addition, as h_{bed} increases, q_e also increases. Other researchers observed similar behaviors too [48, 62].

In continuous conditions, q_e is reduced compared to batch conditions, because in batch conditions, by throwing the adsorbent directly into the solution, full transfer is achieved with full contact. While experimenting on the column, there is a loss as there is a limited contact time.

4.2. Model Studies on Fixed Bed Adsorption Column

4.2.1. Application of Thomas model

The graphs constructed for Thomas model for different parameters are given in Figures 4.5-4.7. The figures demonstrated that there was an appropriate match between the experimental points and the estimated normalized concentration.

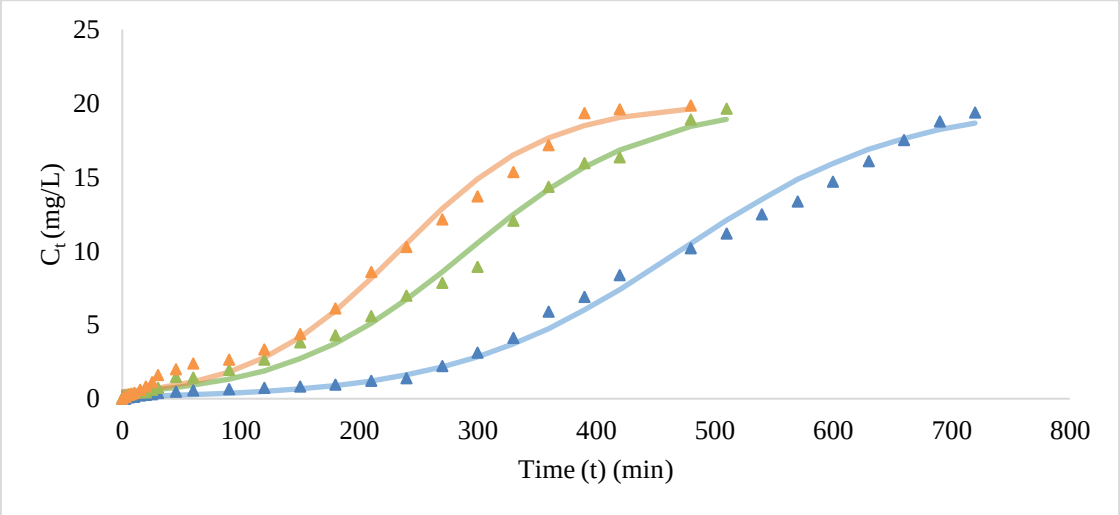

Figure 4. 5. Model fit of breakthrough data to Thomas model for change in Q at h_{bed}=2 cm, C_0=20 ppm (Triangles in blue, green and orange represent Q; 2.5, 5, 7.5 ml/min respectively, crosses represent model fits in the same order)

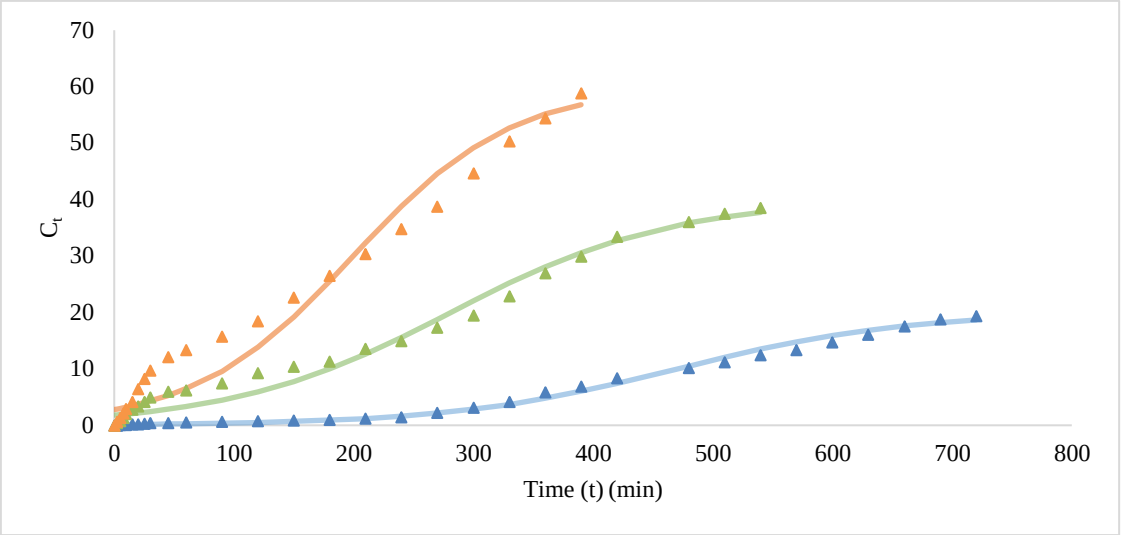

Figure 4. 6. Model fit of breakthrough data to Thomas model for change in C_0, at h_{bed}=2 cm, Q=2.5 ml/min (Triangles in blue, green and orange represent 20, 40 and 60 ppm respectively, crosses represent model fits in the same order)

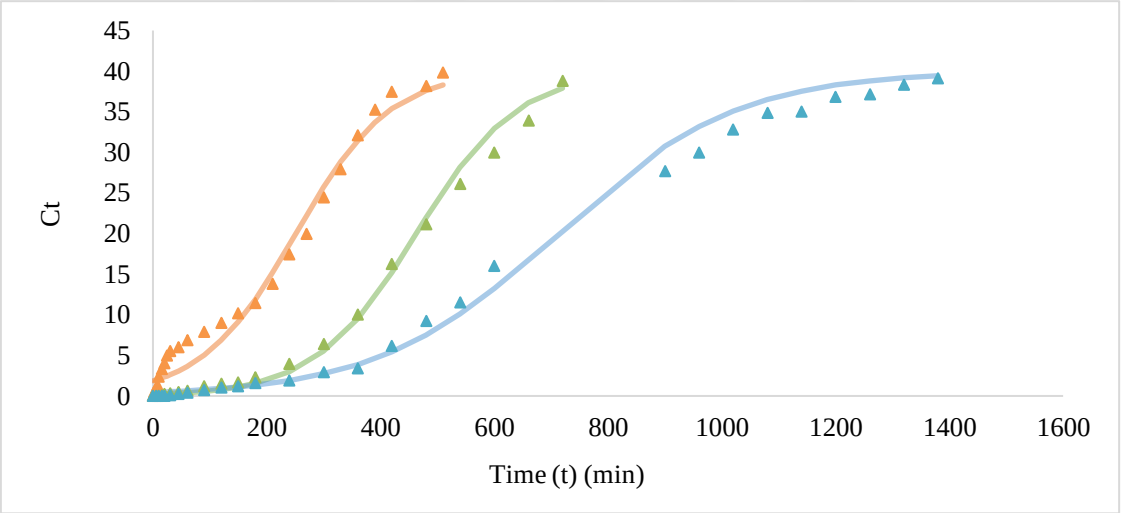

Figure 4. 7. Model fit of breakthrough data to Thomas model for change in h_{bed}, at Q=5 ml/min, C_0=40 ppm (Triangles in blue, green and orange represent 6 ,4 and 2 cm respectively, crosses represent model fits in the same order)

k_{Th}, q_0 values are listed in Table 4.4. It is clear from reviewing, the values of q_0 typically increased with an increase in the value of Q, h_{bed} and C_0. The q_0 value increased with the increase of the flow rate, which showed opposite trend with the q_e value (Table 4.1).

The gap between experimental and calculated values became more obvious as the flow rate increased. It can be concluded that prediction of q_0 with the Thomas model is inaccurate in the continuous adsorption of chromate upon H-CS/PVA. Also high differences between calculated breakthrough time from the model ($t_{b,cal}$) and experimental breakthrough time ($t_{b,exp}$) can be clearly seen from Table 4.4.

The k_{Th} increased with increased Q and decreased h_{bed} which indicated that the diffusional resistance in the liquid layer was comparable to intraparticle diffusivity. Thomas model is based on the assumption that the external and internal diffusions are not the rate limiting step [63], and thus the result is in accordance with theoretical assumption.

The predicted BCs for the Thomas model (Figures 4.5-4.7) are deficient in predicting the initial part of the breakthrough curve. This was due to the errors in the prediction of effluent concentration for time equals to zero.

Table 4. 4. Thomas parameters for the uptake of chromium onto H-CS/PVA

C_o (mg/l)	Q (ml/min)	h_{bed} (cm)	k_{Th} (ml/mg min)	q_0 (mg/g)	$t_{b,cal}$ (min)	$t_{b,exp}$ (min)	ε (%)
20	2.5	2	0.53	5.45	263	250	5.20
20	5	2	0.67	6.77	127	60	111.67
20	7.5	2	0.80	8.11	96	40	140
40	2.5	2	0.27	6.49	77	25	208
60	2.5	2	0.25	6.93	54	20	170
40	5	2	0.30	11.66	68	45	51.11
40	5	4	0.28	13.07	267	180	48.33
40	5	6	0.16	14.17	368	240	53.33

4.2.2. Application of the Adams-Bohart model

The graphs constructed for the Adams-Bohart model for different parameters are shown in Figures 4.8-4.10.

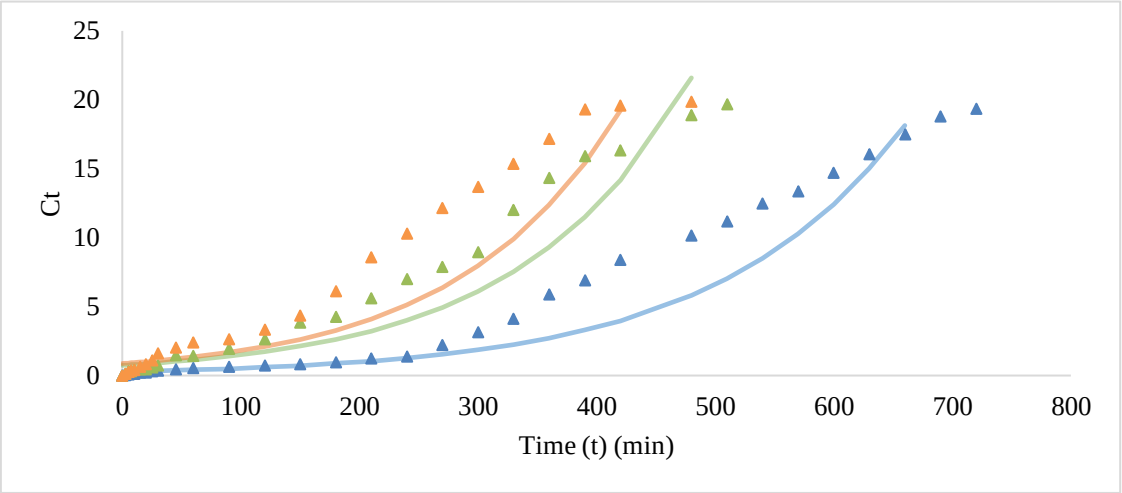

Figure 4. 8. Model fit of breakthrough data to Adams-Bohart model for change in Q at h_{bed}=2 cm, C_0=20 ppm (Triangles in blue, green and orange represent 2.5, 5, 7.5 ml/min respectively, crosses represent model fits in the same order)

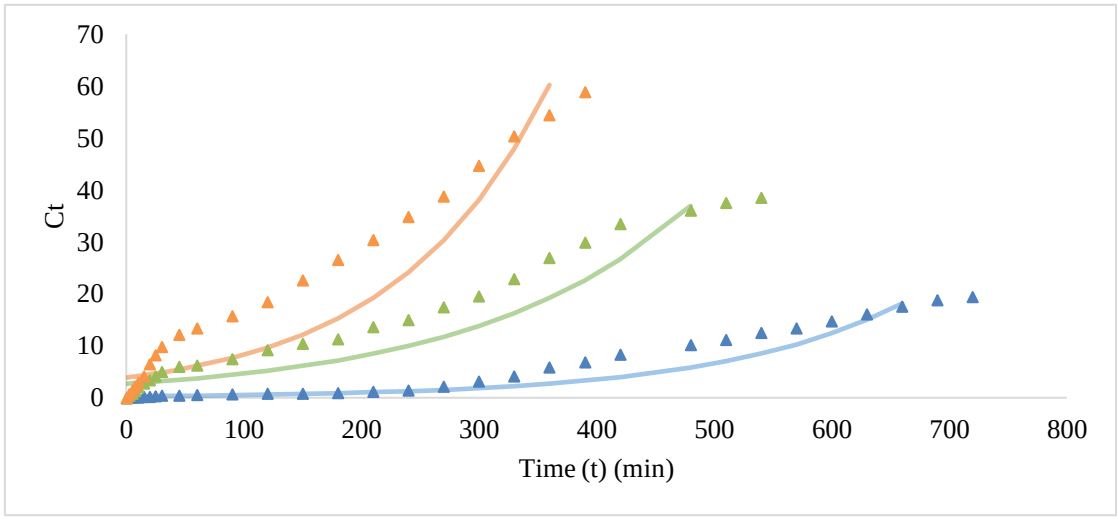

Figure 4. 9. Model fit of breakthrough data to Adams-Bohart model for change in C_0 at h_{bed}=2 cm, Q=2.5 ml/min (Triangles in blue, green and orange represent 20,40 and 60 ppm respectively, crosses represent model fits in the same order)

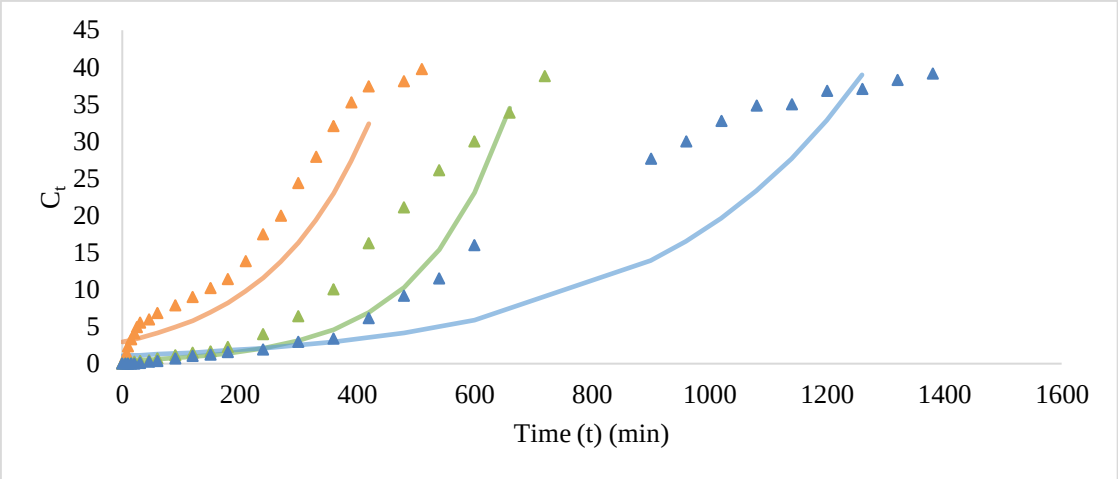

Figure 4. 10. Model fit of breakthrough data to Adams-Bohart model for change in h_{bed}, at Q=5 ml/min, C_0=40 ppm (Triangles in blue, green and orange represent 6,4 and 2 cm respectively, crosses represent model fits in the same order)

Model parameters which were calculated are listed in Table 4.5. Table shows that, in the adsorption of Cr (VI), k_{AB} values decrease but N_0 values increase with the increase in C_0 and Q. However, this model could not provide a good match between experimental data and the predicted concentrations. Also differences between the $t_{b,cal}$ and $t_{b,\,exp}$ values were higher than other studied models.

Table 4. 5. Adams-Bohart parameters for the uptake of chromium on H-CS/PVA

C_o (mg/l)	Q (ml/min)	h_{bed} (cm)	k_{AB} (x 10^{-4} l/mg min)	N_0 (mg/l)	$t_{b,cal}$ (min)	$t_{b,exp}$ (min)	ε (%)
20	2.5	2	0.00032	9329.5	316	250	26.40
20	5	2	0.00035	12958.5	140	60	133.33
20	7.5	2	0.00037	17629.6	114	40	185
40	2.5	2	0.00014	13664.7	83	25	232
60	2.5	2	0.00013	14896.7	64	20	220
40	5	2	0.00014	25246.8	46	45	2.22
40	5	4	0.00017	18842.5	343	180	90.56
40	5	6	0.000072	23371.1	470	240	95.83

4.2.3. Application of the Yoon-Nelson model

The graphs constructed for the Adams-Bohart model for different parameters are shown in Figures 4.11-4.13.

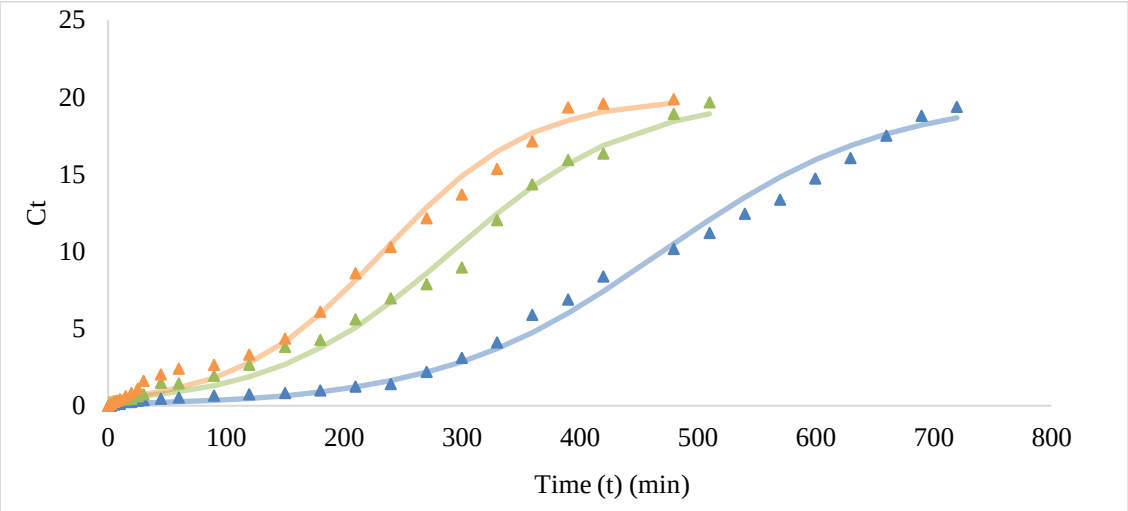

Figure 4. 11. Model fit of breakthrough data to Yoon-Nelson model for change in Q at h_{bed}=2 cm, C_0=20 ppm (Triangles in blue, green and orange represent 2.5, 5, 7.5 ml/min respectively, crosses represent model fits in the same order)

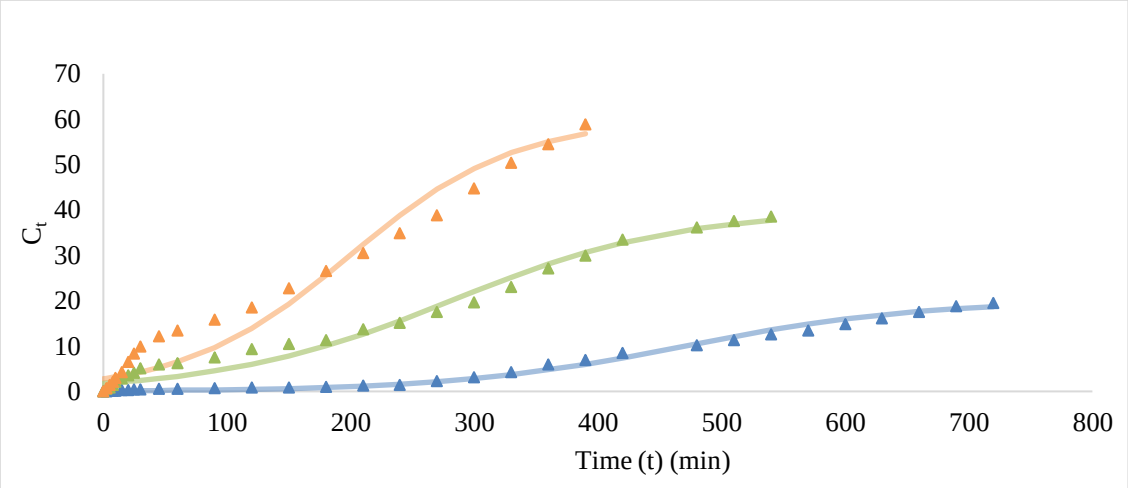

Figure 4. 12. Model fit of breakthrough data to Yoon-Nelson model for change in C_0 at h_{bed}=2 cm, Q=2.5 ml/min (Triangles in blue, green and orange represent 20,40 and 60 ppm respectively, crosses represent model fits in the same order)

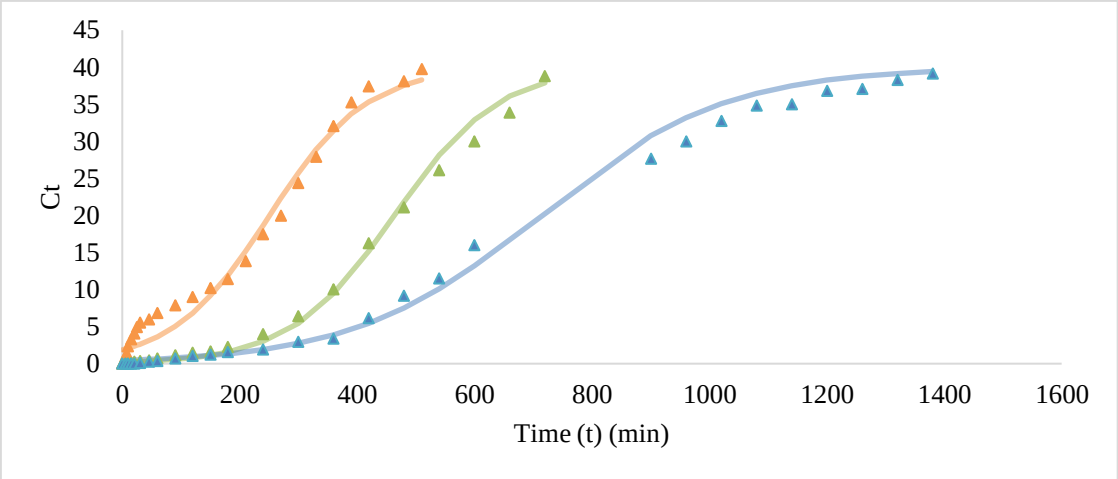

Figure 4. 13. Model fit of breakthrough data to Yoon-Nelson model for change in h_{bed}, at Q=5 ml/min, C_0=40 ppm (Triangles in blue, green and orange represent 6,4 and 2 cm respectively, crosses represent model fits in the same order)

The findings in Table 4.6. and graphs indicates that the τ_{cal} values that were predicted by the Yoon and Nelson model were very closely to those which were expected based on the outcomes of experiments. Percent deviation (ε) between experimental (τ_{exp}) and calculated (τ_{cal}) time for the breakthrough are given in Table 4.6.

Table 4. 6. Yoon-Nelson parameters for the uptake of chromium on H-CS/PVA

C_o (mg/l)	Q (ml/min)	h_{bed} (cm)	k_{YN} (l/min)	τ_{cal} (min)	τ_{exp} (min)	ε (%)
20	2.5	2	0.0106	470.3	480	2.02
20	5	2	0.0131	291.8	310	5.87
20	7.5	2	0.0161	233.5	238	1.89
40	2.5	2	0.0108	281.1	300	6.30
60	2.5	2	0.0151	199.7	200	0.15
40	5	2	0.0120	251.2	270	6.96
40	5	4	0.0113	463.2	470	1.45
40	5	6	0.0063	711.1	701	1.44

As can be seen in Table 4.6, an increase in Q led to an increase in k_{YN} but a decrease in time for required 50% breaktrough. A similar trend was observed with the increase in concentration. However the opposit tendency was recorded with the increase in bed depth. The validity of this model has been demonstrated by the fact that the model and the experimental data are quite comparable to one another.

4.2.4. Application of the BDST model

BDST model can be used for determination of column design parameters. Table 4.7 lists the BDST constants, k_{BDST} and N_0, calculated using non-linear form of the Eqn 2.9.

Table 4. 7. The BDST parameters for the uptake of chromium on H-CS/PVA

C_o (mg/l)	Q (ml/min)	h_{bed} (cm)	k_{BDST} (ml/mg.min)	N_0 (mg/l)
20	2.5	2	0.00053	6496
20	5	2	0.00067	4031
20	7.5	2	0.00080	3226
40	2.5	2	0.00027	7766
60	2.5	2	0.00025	8275
40	5	2	0.00030	13879
40	5	4	0.00028	12797
40	5	6	0.00016	13095

Experimental results were applied to the BDST model to determine adsorption capacities (N_0) and kinetic constants (k_{BDST}). Breakthrough service time (t_b, min) against bed height (h_{bed}, cm) graphs at C_t/C_0 of 0.1 value is shown in Figure 4.14..

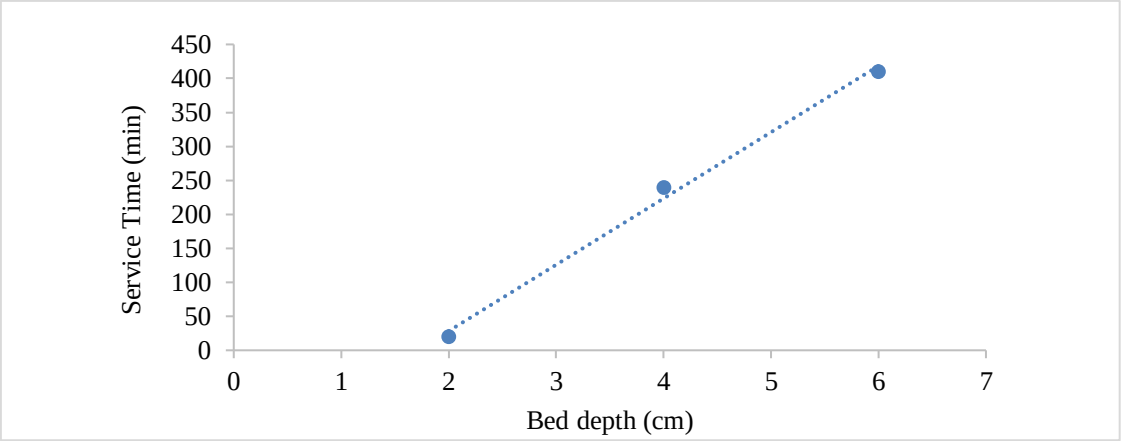

Figure 4. 14. BDST equation line for Cr (VI) adsorption at C_0 = 40 mg/l, Q = 5 ml/min, C_t/C_0 = 0.1)

The constants of the model are evaluated from the slope and intercept of the line are given in Table 4.8.

Table 4. 8. BDST model parameters for the adsorption of chromium on H-CS/PVA at C_0 = 40 mg/l, Q = 5 ml/min

C_t/C_0	a (min/cm)	b (min)	k_{BDST} (ml/mg.min)	N_0 (mg/L)	Z_0 (cm)	R^2
0.1	97.5	166.7	0.013	24075	1.7	0.995

It was determined that at t_b=0, the required minimum bed depth should not be less than 1.7 cm for the adsorption of Cr (VI) to H-CS-PVA so that the exit concentration does not exceed the desired breakpoint concentration. The BDST equation obtained at a flow rate of 5 mL/min and an initial concentration of 40 mg/L, at other flow rates and other initial Cr (VI) concentration was used to estimate the performance of the adsorbent. Table 4.9. shows parameters for different C_0 and Q values.

Table 4. 9. Estimated values from BDST model constants at a new Q or a new C_0 value

C_t/C_0	a' (min/cm)	b' (min)	t_{cal} (min)	t_{exp} (min)	ε (%)
Q = 5 ml/min, C_0'= 20 mg/l					
0.1	195	333.8	56.2	92	38.9
Q' = 2.5 ml/min, C_0 = 40 mg/l					
0.1	195	166.7	223.3	25	793.3

When As can be seen from Table 4.9, there is sigificant difference between the service times of the column determined experimentally and calculated with the BDST model.

4.3. Error Function Analysis

Error function analysis was employed for determining the most suitable model. Table 4.10 lists the results of the error studies. For model fitting, Chi-Square Test (X^2), average relative error (ARE), and Marquardt's percent standard deviation (MPSD) were applied. The best fitted model must have lower X^2, ARE, and MPSD value. The outcomes led to the conclusion that the Thomas, BDST and Yoon-Nelson models provided the similar values and most accurate representation for Cr (VI) adsorption in continous system towards Adams-Bohart values.

The linearity for the three models, including BDST, Thomas, and Yoon–Nelson, depict in same expression. It can be said that, the characteristic parameters related to these models differ but all three models predict C_t values for certain data sets that are basically identical. Consequently, their other statistical parameters, X^2, ARE, MPSD values are similar, as illustrated in Table 4.10.

However, the key and distinctive feature for Yoon–Nelson model is the time for 50% breakthrough (τ). According to the values listed in Table 4.6, a good correlation exists between τ values calculated with the model and determined experimentally. On the other hand the distinctive characteristics of Thomas and BDST models could not provide such a level of precision. Concordantly, the Yoon–Nelson model was selected as the most accurate amongst the studied models.

Table 4. 10. Models' error function values for Cr (VI) adsorption by H-CS/PVA

			Thomas			Adams-Bohart			Yoon-Nelson			BDST		
Q (1)	**C_0** (2)	**Z** (3)	X^2	ARE	MPSD	X^2	ARE	MPSD	X^2	ARE	MPSD	X^2	ARE	MPSD
2.5	20	2	3.1	43.2	0.60	23.1	68.4	0.79	3.1	43.2	0.60	3.1	43.2	0.68
5	20	2	2.8	23.9	0.39	20.0	45.6	0.58	2.8	23.9	0.39	2.8	23.9	0.51
7.5	20	2	4.2	30.5	0.46	31.9	58.1	0.69	4.2	30.5	0.46	4.2	30.5	0.58
2.5	40	2	15.8	33.8	0.48	47.3	54.0	0.63	15.8	33.8	0.48	15.8	35.2	0.62
2.5	60	2	30.4	38.9	0.52	70.3	54.9	0.66	30.4	38.9	0.52	30.4	38.9	0.66
5	40	2	14.8	31.8	0.47	48.8	53.8	0.64	14.8	31.8	0.47	14.8	31.8	0.59
5	40	4	4.2	45.8	0.58	36.3	68.1	0.77	4.2	45.8	0.58	4.2	45.9	0.71
5	40	6	3.9	20.1	0.30	58.8	53.8	0.64	3.9	20.1	0.30	3.9	24.8	0.48

(1)(ml/min), (2)(mg/l), (3)(cm)

4.3. Characterization Analysis

4.3.1. SEM and SEM-EDX analysis

The morphology of the H-CS/PVA beads was analyzed both before and after adsorption by using SEM. Figure 4.15 shows the SEM results.

It can be seen from the Fig. 4.15.a that the form of adsorbents is oval-shaped and surface morphology of H-CS/PVA is homogeneous before adsorption. The lumpy surface of unloaded H-CS/PVA, seen in Fig. 4.15.b, formed voids and protrusions on the adsorbent that enabled mass transfer. It was observed that the cavities in the adsorbent were filled with after chromium adsorption (Fig. 4.15.d). In addition, shiny small adsorbate layers covering some parts of the bead surface were formed on the saturated H-CS/PVA (Fig 4.15.d).

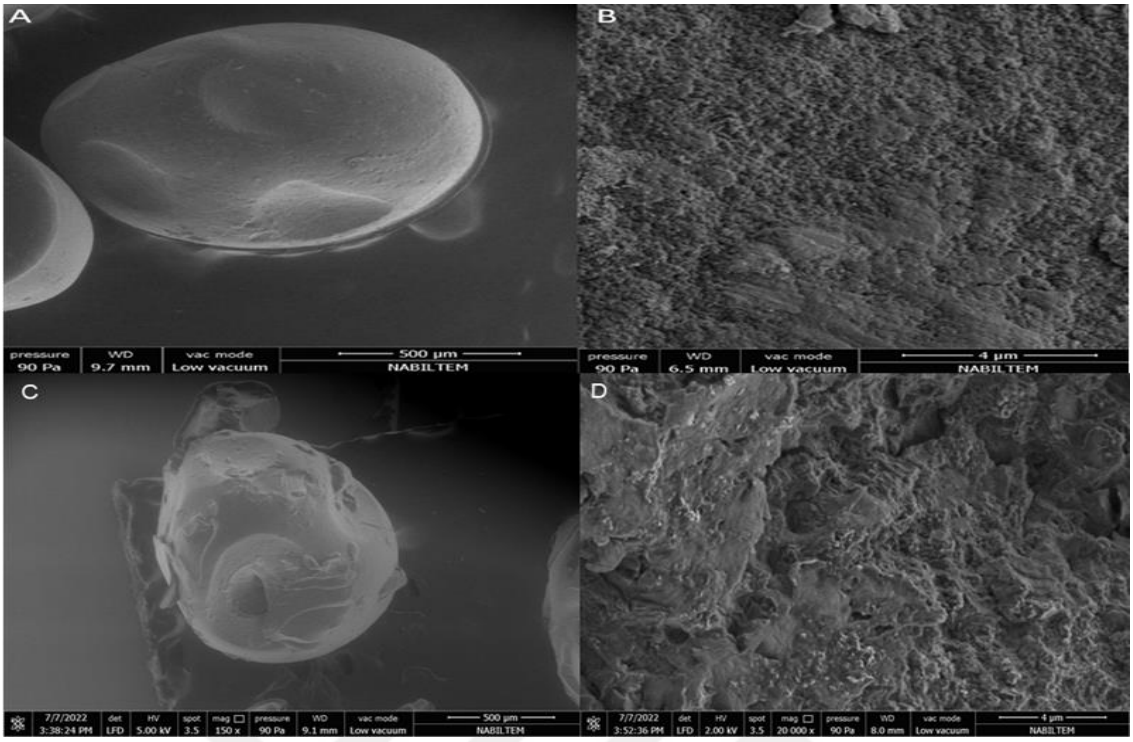

Figure 4. 15. SEM images of H-CS/PVA a) before the adsorption at 150 magnification, b) before the adsorption at 20000 magnification, c) after the adsorption at 150 magnification, d) after the adsorpiton at 20000 magnification

Thanks to SEM analysis, physical differences in the structure of the adsorbent before and after adsorption were observed. SEM-EDX analysis was performed to figure out the chemical composition of the material; the findings are shown in Table 4.11 and Figure 4.16.

Table 4. 11. SEM-EDX results of CS-PVA adsorbent

Element	Weight % (Unloaded H-CS/PVA)	Weight % (Loaded H-CS/PVA)
C	51.01	41.263
N	5.71	6.107
O	43.28	51.6
Cr	-	1.03
Total	100	100

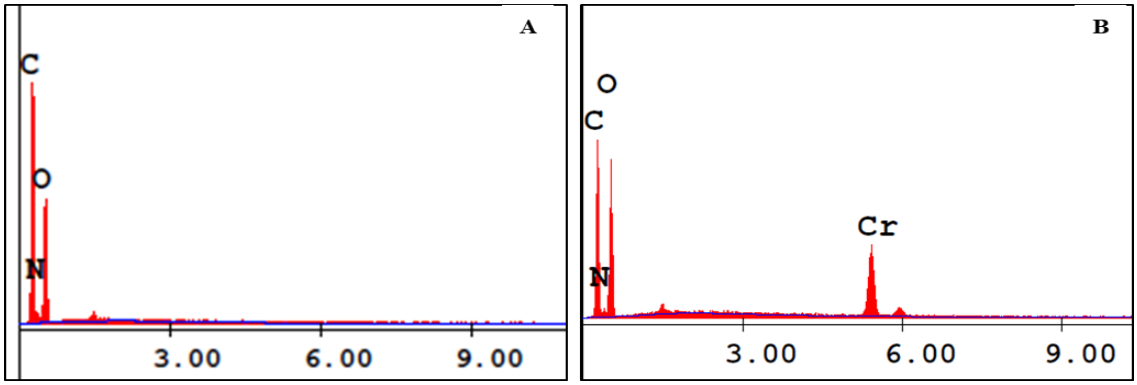

Figure 4. 16. SEM-EDX graphs of H-CS/PVA (A: unloaded H-CS/PVA, B: loaded H-CS/PVA)

Based on the comparison of SEM-EDX analysis before and after adsorption, the presence of chromium after adsorption has been clearly demonstrated in Figure 4.16.b. The mass percentage of Cr was detected to be in the order of 1%, which provided a proof of the adsorption of Cr(VI) occurring in the active sites on the surface.

4.3.2. FTIR analysis

The FTIR spectrum of the different functionalities obtained before and after the adsorption of H-CS/PVA are given in Figure 4.17. Therefore, the H-CS/PVA spectrum contained all the peaks typically associated with CS and PVA structures.

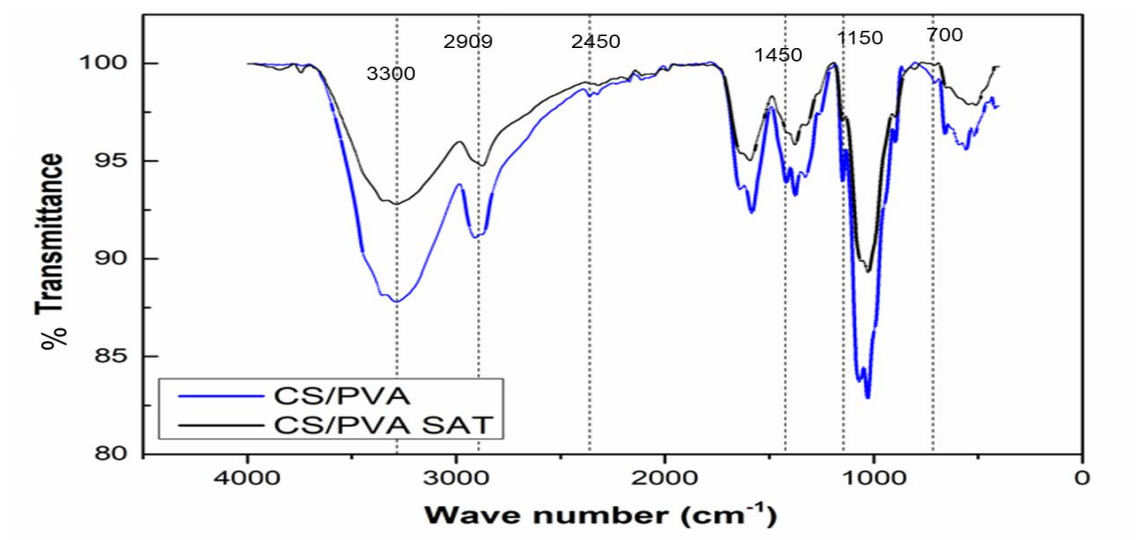

Figure 4. 17. FTIR spectrum of H-CS/PVA beads

The N-H and O-H vibrations in chitosan and the hydroxyl groups in PVA cause the peak at 3300 cm^{-1}. The peak at appearing 1450 cm^{-1} indicates amide stretches. And the peak 1000 cm-1 corresponded to the stretching vibrations of the strong C-O-C and CO groups. The bands at 1000 and 1060 cm^{-1} that originated from symmetric and asymmetric C-O-C stretching vibrations in the oxygen bridge of chitosan remained unchanged after the adsorption. Furthermore, a protonated amine group NH^{3+} appeared as a new peak at eleven hundred, which was favorable for anion adsorption [10, 64, 65].

4.3.3. BET analysis

The surface area, overall pore volume and pore distribution of the fabricacted beads were analyzed with N_2 adsorption. According to the results, obtained with 99% precision, the surface area and overall pore volume of the synthesized beads were determined as 2.96 m^2/g and 0.35 cm^3/g, respectively. The characterization of fully loaded beads was also accomplished to discuss the possible mechanism dominating the adsorption process. According to the results, the isotherms of N_2 adsorption/desorption on fully loaded H-CS/PVA was comparably different than that of pristine H-CS/PVA, which implied that Cr(VI) was fixed at the active sites inside the pores. The alteration of the specific surface area was even more obvious which suggested that fixation of Cr(VI) at the surface active sites had a greater contribution than adsoption in the pores.

5. CONCLUSIONS

In this study, the potential of H-CS/PVA was analyzed in a continuous adsorption column as an adsorbent for Cr (VI). This novel adsorbent was previously synthesized in another study and its efficacy for Cr (VI) adsorption was proven under batch conditions. However, continuous adsorption in a fixed bed adsorption column is anticipated to differ due to a number of factors involved in the column design, such as, contact time and packing height. In this regard, the effects of column parameters, namely, flow rate, initial concentration and height of packing, was investigated in detail using one factor at a time approach and in each case the effluent concentration was monitored to obtain breakthough curves. The breakthrough times and the curve shapes were inspected to evaluate the plausible dominant mechanism for mass transfer and to calculate related parameters.

The flow rate (Q) was varied within the range of 2.5-7.5 mL/min. Substantial decreases in both the saturation and the breakthrough times were recorded in the order of increasing flow rate. A similar trend was observed in the removed percentage of chromium ions. In other words, a low flow rate was necessary to achieve satisfactory adsorption performance in the column.

The feed concentration of Cr (VI) was studied at three different levels within the range 20-60 ppm. Increased influent concentration at a fixed flow rate and bed height led to shortened the breakthrough time and deteriorated the well known S-shape of the curve. Yet, increases in C0 were in favor of adsorption capacity.

Packing height was also studied at three levels as 2, 4 and 6 cm. As anticipated, increasing hbed improved chromium removal mainly due to increased number of active sites for adsorption. The exhaustion and breakthrough time were also extended as hbed was increased.

Minimum removal was detected as 23.12% at the flow rate of 2.5 ml/min, inlet concentration of 20 ppm and bed height of 2 cm. Meanwhile, maximum removal reached as high as 64.2 % at flow rate of 5 ml/min, inlet concentration of 40 ppm and bed height of 6 cm. The maximum adsorption capacity H-CS/PVA adsorbent in a fixed bed adsorption column was determined as 15.53 mg/g. t is possible that this potential might be improved further via analyzing the combined effect of flow rate, Cr (VI) concentration at the inlet and bed depth with the help of statistical experimental design techniques.

Column kinetic parameters were evaluated by applying Thomas, Adams–Bohart, Yoon-Nelson, and BDST models. Out of the studied models, Yoon-Nelson model was selected to be the most precise one for describing the adsorption of Cr (VI) onto H-CS/PVA in continuous system. Yoon-Nelson model provided the highest resemblence for breakthrough times and dynamic concentration of effluent thus was the most accurate model for description of the dynamic behavior of the column. Moreover, the lowest error fuction values (X^2, ARE, MPSD) were calculated for the Yoon-Nelson model, which further verified its accuracy.

BDST model was used for determination of column design parameters such as critical bed depth and breakthrough time. The linearized model provided high correlation coefficient (R^2>0.99), yet, estimation of breakthrough times based on calculated model constants for other experimental conditions was fairly inaccurate.

All these results emphasized upon the applicability of H-CS/PVA the packing material in a continuously operated fixed-bed adsorption column. Still, all the enclosed data were obtained using synthetic wastewater and thus, it is suggested to evaluate and validate the adsorbent performance with real wastewater.

6. REFERENCES

1. Briffa, J., E. Sinagra, and R. Blundell, Heavy metal pollution in the environment and their toxicological effects on humans. Heliyon, 2020. 6(9): p. e04691.
2. Mohamed Nageeb, R., Adsorption Technique for the Removal of Organic Pollutants from Water and Wastewater, in Organic Pollutants, M.N. Rashed, Editor. 2013, IntechOpen: Rijeka. p. Ch. 7.
3. Ho, S., Low-Cost Adsorbents for the Removal of Phenol/Phenolics, Pesticides, and Dyes from Wastewater Systems: A Review. 2022. 14(20): p. 3203.
4. Zia, Q., et al., A Review on Chitosan for the Removal of Heavy Metals Ions. Journal of Fiber Bioengineering and Informatics, 2019. 12: p. 103-128.
5. Ben Halima, N., Poly (vinyl alcohol): review of its promising applications and insights into biodegradation. 2016. 6(46): p. 39823-39832.
6. Anitha, T., P. Senthil Kumar, and K. Sathish Kumar, Binding of Zn(II) ions to chitosan–PVA blend in aqueous environment: Adsorption kinetics and equilibrium studies. 2015. 34(1): p. 15-22.
7. Sahebjamee, N., et al., Removal of Cu2+, Cd2+ and Ni2+ ions from aqueous solution using a novel chitosan/polyvinyl alcohol adsorptive membrane. 2019. 210: p. 264-273.
8. Li, L., et al., Preparation of polyvinyl alcohol/chitosan hydrogel compounded with graphene oxide to enhance the adsorption properties for Cu (II) in aqueous solution. 2015. 22(8): p. 1-10.
9. Mihaela Predescu, A., et al., Adsorption of lead (II) from aqueous solution using chitosan and polyvinyl alcohol blends. 2019. 52(15): p. 2365-2392.
10. Aydin, Y.A., Fabrication of chitosan/polyvinyl alcohol/amine modified carbon nanotube composite films for rapid chromate removal. Journal of Applied Polymer Science, 2021. 138(18): p. 50339.
11. Demirci Ülke, A.S., Cr (VI) removal from wastewaters using chitosan-polyvinyl alcohol beads. 2021, Marmara University, Institute Of Graduate Studies In Pure And Applied Sciences, : İstanbul,Türkiye.
12. Wardhono, E.Y., et al., Modification of Physio-Mechanical Properties of Chitosan-Based Films via Physical Treatment Approach. 2022. 14(23): p. 5216.
13. Suflet, D.M., et al., Dual Cross-Linked Chitosan/PVA Hydrogels Containing

Silver Nanoparticles with Antimicrobial Properties. 2021. 13(9): p. 1461.
14. Yi, R., et al., Mild hydrothermal preparation of millimeter-sized carbon beads from chitosan with significantly improved adsorption stability for Cr(VI). Chemical Engineering Research and Design, 2020. 156: p. 43-53.
15. Gazete, R.B.B., Su Kirliliği Kontrolü Yönetmeliği. 2004. 25687.
16. Nurbaş Nourbakhsh, M., et al., Biosorption of Cr6+, Pb2+ and Cu2+ ions in industrial waste water on Bacillus sp. Chemical Engineering Journal, 2002. 85(2): p. 351-355.
17. Özdede, A., Polipirol/kitosan kompozit polimeri kullanılarak sulu çözeltİlerden bazı ağır metallerin giderim şartlarının incelenmesi. Yüksek Lisans Tezi, Dumlupınar Üniversitesi, Fen Bilimleri Enstitüsü, Kütahya, Türkiye, 2013.
18. Saravanan, A., et al., Effective water/wastewater treatment methodologies for toxic pollutants removal: Processes and applications towards sustainable development. Chemosphere, 2021. 280: p. 130595.
19. Sezer, K., Atıksulardaki Kadmiyum(II) ve Nikel(II) İyonlarının Tekli ve İkili Karışımlarının Kitosana, Kile ve Kitosan-Kil Kompozitine Adsorpsiyonunun Kesikli ve Sürekli Sistemlerde İncelenmesi, in Doktora Tezi, Hacettepe Üniversitesi, Fen Bilimleri Enstitüsü, Ankara, Türkiye. 2015.
20. Kahvecioğlu, Ö., et al., Metallerin çevresel etkileri-I. 2003. 136: p. 47-53.
21. Atieh, M.A., et al., Removal of Chromium (III) from Water by Using Modified and Nonmodified Carbon Nanotubes. Journal of Nanomaterials, 2010. 2010: p. 232378.
22. Mohan, D., K.P. Singh, and V.K. Singh, Trivalent chromium removal from wastewater using low cost activated carbon derived from agricultural waste material and activated carbon fabric cloth. Journal of Hazardous Materials, 2006. 135(1): p. 280-295.
23. Fang, J., et al., Cr (VI) removal from aqueous solution by activated carbon coated with quaternized poly (4-vinylpyridine). 2007. 41(13): p. 4748-4753.
24. IARC, International Agency for Research on Cancer, Arsenic, metals, fibres, and dusts: IARC monographs on the evaluation of carcinogenic risks to humans, Volume 100C. 2011, International Agency for Research on Cancer Lyon. p. 164.
25. Vaiopoulou, E. and P. Gikas, Regulations for chromium emissions to the aquatic

environment in Europe and elsewhere. Chemosphere, 2020. 254: p. 126876.
26. Sundaram, S. and P. Raghavan, Chromium-VI reagents: synthetic applications. 2011: Springer Science & Business Media.
27. Tumolo, M., et al., Chromium pollution in European water, sources, health risk, and remediation strategies: An overview. International Journal Of Environmental Research Public Health2020. 17(15): p. 5438.
28. Sayid, D., Polivinil alkol ve karbon nanotüp ile modifiye edilen kitosan kullanılarak atık sulardan Cr(VI) giderimi. 2018, İstanbul Teknik Üniversitesi, Fen Bilimler Enstitüsü: İstanbul, Türkiye.
29. Fu, F. and Q. Wang, Removal of heavy metal ions from wastewaters: a review. J Environ Manage, 2011. 92(3): p. 407-18.
30. Azimi, A., et al., Removal of heavy metals from industrial wastewaters: a review. ChemBioEng Reviews
2017. 4(1): p. 37-59.
31. Zhang, Y. and X. Duan, Chemical precipitation of heavy metals from wastewater by using the synthetical magnesium hydroxy carbonate. Water Science and Technology, 2020. 81(6): p. 1130-1136.
32. Rene, E.R., et al., Sustainable Heavy Metal Remediation: Volume 1: Principles and Processes. Vol. 8. 2017: Springer.
33. Das, T.K. and A. Poater, Review on the Use of Heavy Metal Deposits from Water Treatment Waste towards Catalytic Chemical Syntheses. 2021. 22(24): p. 13383.
34. Lonsdale, H., The growth of membrane technology. Journal Of Membrane Science, 1982. 10(2-3): p. 81-181.
35. Raut, P.A., A. Chahande, and Y. Moharkar, Various techniques for the removal of Chromium and lead from Waste water. Int. J. Emerg. Trend. Eng. Basic Sci.
, 2015. 2(2): p. 64-67.
36. Algieri, C., et al., Arsenic removal from groundwater by membrane technology: Advantages, disadvantages, and effect on human health. Groundwater for Sustainable Development, 2022. 19: p. 100815.
37. Gunatilake, S., Methods of Removing Heavy Metals from Industrial Wastewater. Journal of Multidiciplinary Engineering Science Studies, 2015. 1.
38. Barakat, M.A., New trends in removing heavy metals from industrial wastewater.

Arabian Journal of Chemistry, 2011. 4(4): p. 361-377.

39. Sarıkaya, Y., Fizikokimya, Genişletilmiş 4. Baskı. Gazi Kitapevi, Ankara, Türkiye, 2003.
40. Smith, J.M., Chemical engineering kinetics. 1970.
41. Sıvri, N., Sabit Yataklı Kolonda Atık Sulardan Hekzavalent Krom Gideriminin İncelenmesi, in Yüksek Lisans Tezi, İstanbul Teknik Üniversitesi, Fen Bilimleri Enstitüsü, İstanbul,Türkiye. 2015.
42. Araç, E., Sulu çözeltideki kurşun ve bakır iyonlarının sepiyolit ile adsorpsiyonu, in Fen Bilimleri Enstitüsü. 2014, İstanbul Teknik Üniversitesi, İstanbul, Türkiye.
43. Zarghami, S., M. ahmadzadeh tofighy, and T. Mohammadi, Adsorption of Zinc and Lead Ions From Aqueous Solutions Using Chitosan/Polyvinyl Alcohol Membrane Incorporated via Acid Functionalized Carbon Nanotubes. Journal of Dispersion Science and Technology, 2014. 36: p. 150527103417002.
44. Kas, H.S., Chitosan: Properties, preparations and application to microparticulate systems. Journal of Microencapsulation, 1997. 14(6): p. 689-711.
45. Wan Ngah, W.S., L.C. Teong, and M.A.K.M. Hanafiah, Adsorption of dyes and heavy metal ions by chitosan composites: A review. Carbohydrate Polymers, 2011. 83(4): p. 1446-1456.
46. Yang, J.M., et al., Evaluation of chitosan/PVA blended hydrogel membranes. Journal of Membrane Science, 2004. 236(1): p. 39-51.
47. Chauhan, D. and N. Sankararamakrishnan, Modeling and evaluation on removal of hexavalent chromium from aqueous systems using fixed bed column. J Hazard Mater, 2011. 185(1): p. 55-62.
48. Golie, W.M. and S. Upadhyayula, Continuous fixed-bed column study for the removal of nitrate from water using chitosan/alumina composite. Journal of Water Process Engineering, 2016. 12: p. 58-65.
49. Nassar, N., Iron Oxide Nanoadsorbents for Removal of Various Pollutants from Wastewater: An Overview. 2012. p. 81-118.
50. Vukojević Medvidović, N., et al., Removal of lead ions by fixed bed of clinoptilolite – The effect of flow rate. Microporous and Mesoporous Materials, 2007. 105(3): p. 298-304.
51. Chowdhury, Z., S.B. Abd Hamid, and S. Zain, Evaluating Design Parameters for

Breakthrough Curve Analysis and Kinetics of Fixed Bed Columns for Cu(II) Cations Using Lignocellulosic Wastes. BioResources, 2014. 10.

52. Yoon, Y.H. and J.H.J.A.i.h.a.j. Nelson, Application of gas adsorption kinetics I. A theoretical model for respirator cartridge service life. 1984. 45(8): p. 509-516.
53. Bohart, G. and E.J.J.o.t.A.c.s. Adams, Some aspects of the behavior of charcoal with respect to chlorine. 1920. 42(3): p. 523-544.
54. Aksu, Z. and F.J.P.b. Gönen, Biosorption of phenol by immobilized activated sludge in a continuous packed bed: prediction of breakthrough curves. 2004. 39(5): p. 599-613.
55. Baral, S.S., et al., Removal of Cr(VI) by thermally activated weed Salvinia cucullata in a fixed-bed column. Journal of Hazardous Materials, 2009. 161(2): p. 1427-1435.
56. Han, R., et al., Characterization and properties of iron oxide-coated zeolite as adsorbent for removal of copper(II) from solution in fixed bed column. Chemical Engineering Journal, 2009. 149(1): p. 123-131.
57. Lin, X., et al., Estimation of fixed-bed column parameters and mathematical modeling of breakthrough behaviors for adsorption of levulinic acid from aqueous solution using SY-01 resin. Separation and Purification Technology, 2017. 174: p. 222-231.
58. Liao, P., et al., Adsorption of tetracycline and chloramphenicol in aqueous solutions by bamboo charcoal: A batch and fixed-bed column study. Chemical Engineering Journal, 2013. 228: p. 496-505.
59. Leudjo Taka, A., et al., Chitosan nanocomposites for water treatment by fixed-bed continuous flow column adsorption: A review. Carbohydr Polym, 2021. 255: p. 117398.
60. Mondal, S., K. Aikat, and G. Halder, Ranitidine hydrochloride sorption onto superheated steam activated biochar derived from mung bean husk in fixed bed column. Journal of Environmental Chemical Engineering, 2016. 4(1): p. 488-497.
61. Sadaf, S. and H.N. Bhatti, Evaluation of peanut husk as a novel, low cost biosorbent for the removal of Indosol Orange RSN dye from aqueous solutions: batch and fixed bed studies. Clean Technologies and Environmental Policy, 2014. 16(3): p. 527-544.

62. Qaiser, S., A.R. Saleemi, and M. Umar, Biosorption of lead from aqueous solution by Ficus religiosa leaves: Batch and column study. Journal of Hazardous Materials, 2009. 166(2): p. 998-1005.
63. Singha, S. and U. Sarkar, Analysis of the dynamics of a packed column using semi-empirical models: Case studies with the removal of hexavalent chromium from effluent wastewater. Korean Journal of Chemical Engineering, 2015. 32(1): p. 20-29.
64. Supriya Bhatt, S., G. Thakur, and M. Nune, Preparation and characterization of PVA/Chitosan cross-linked 3D scaffolds for liver tissue engineering. Materials Today: Proceedings, 2023.
65. Koosha, M., et al., Physically Crosslinked Chitosan/PVA Hydrogels Containing Honey and Allantoin with Long-Term Biocompatibility for Skin Wound Repair: An In Vitro and In Vivo Study. 2021. 12(4): p. 61.

ATTACHMENTS

ATTACHMENT A : Calibration curve for Cr (VI)

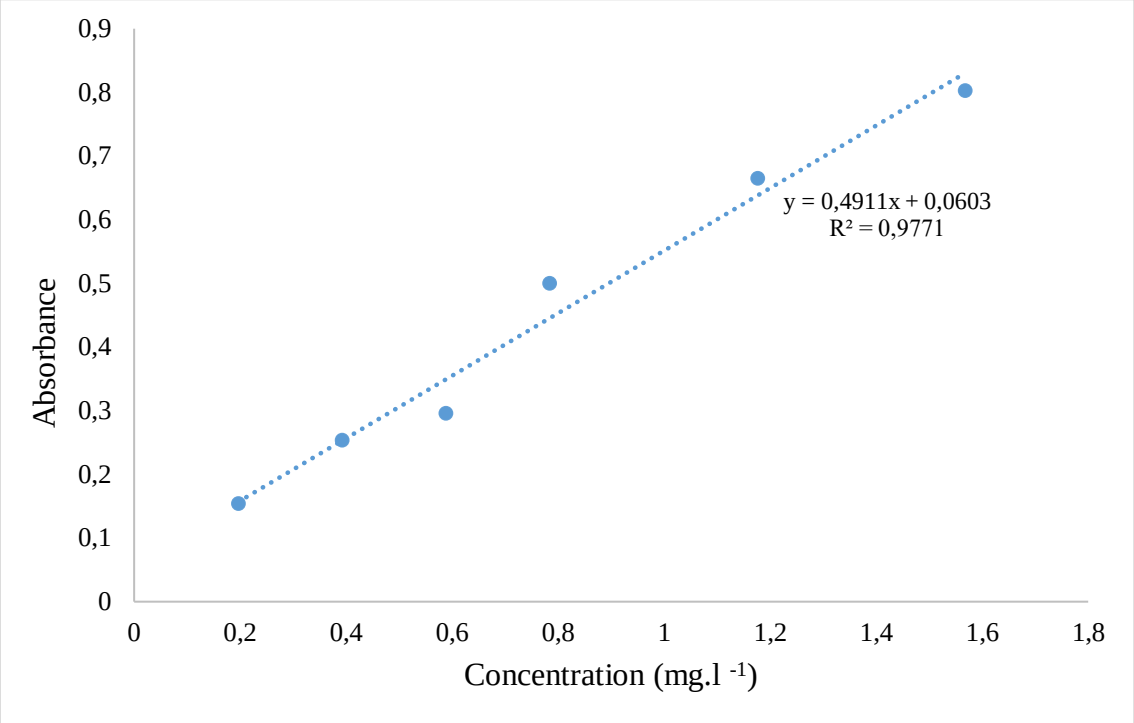

CURRICULUM VITAE

Name – Surname : Eylül KÖSOĞLU

EDUCATION STATUS :

License : 2020, Anadolu University, Chemical Engineering

PUBLICATIONS

1. Kösoğlu E., Aydın .Y.A. (2022), Continuous Adsorption Process For Cr (VI) On Hydrothermally Treated Chitosan/Polyvinyl Alcohol Beads, 9th IUPAC International Conference on Green Chemistry (9th ICGC), 5-9 September, 2022, Athens, Greece (Certificate of Participation – Orally presented)